Master Thesis

Quaternionic Shape Analysis

Thomas Frerix

Master Program
Theoretical and Mathematical Physics

Technische Universität München
Ludwig-Maximilians-Universität München

First reviewer:	Prof. Dr. Daniel Cremers
Second reviewer:	Prof. Dr. Tim Hoffmann
Advisor:	Dr. Emanuele Rodolà
Date of defense:	November 28, 2014

ἀγεωμὲρητος
μηδεὶς
εἰσίτω

Let no one
ignorant of geometry
enter here

Engraved at the door of Plato's Academy in ancient Athens

Preface

This Master thesis summarizes the work during the final project of my Master degree program *Theoretical and Mathematical Physics*, a joint program of the two Munich universities, the Technical University Munich and the Ludwig-Maximilians-University Munich. The work was conducted in the Shape Analysis division of the chair for Computer Vision and Pattern Recognition held by Prof. Dr. Daniel Cremers.

In the process of developing a suitable thesis topic, I was making myself familiar with the work of the Shape Analysis community, which focuses on algorithmically characterizing the geometry of single shapes and comparing the geometry of two or more shapes that are often physical deformations of each other. From a mathematical point of view, the class of deformations considered in this community is mostly that of near isometries. In order to follow the massive amount of recent literature in the field, I pursued a top-down approach as outlined in Chapter 1.2 to arrive at an obviously difficult integrability condition, the Gauß-Mainardi-Codazzi equations (Eq. (1.1)). It was about this time that I came across Keenan Crane's work in Conformal Geometry Processing, which is summarized in his PhD thesis of the same title ([4]). To my surprise at that time, this framework offers a theoretically pleasing and practically feasible formulation of conformal deformations and in particular an integrability condition, which in practice eventually boils down to solving an eigenvalue problem.
Whereas this framework has so far been used in Geometry Processing, the approach taken in this thesis is to my knowledge the first attempt to bring these ideas to the related Shape Analysis community, in the sense that I intend to restrict the class of conformal deformations and to single out the case of *physical deformations*, that is, (near) isometries.
As this framework is based on a surface description by means of quaternions, the present thesis came to its name, *Quaternionic Shape Analysis*.

We begin our investigation by laying the foundation of Quaternionic Shape Analysis in Chapter 2, which offers a technical introduction to quaternions, quaternionic differential forms and quaternionic Hilbert spaces. The emphasis is on *practicality*, as we want to be equipped with a calculus, which we will apply in the remainder of the thesis.
Chapter 3 presents a representation of conformal shape space. As a prerequisite for this definition we introduce *mean curvature half-density* in Chapter 3.1 as a central quantity of the framework

that can be considered as coordinates in conformal shape space. The natural transformation in conformal shape space is *spin transformation* and is outlined in Chapter 3.2. In order to arrive at another surface in shape space via spin transformation an additional *integrability condition* has to be satisfied, which is also outlined in Chapter 3.2 and reformulated as a generalized eigenvalue problem of the central operator of the framework, the *quaternionic Dirac operator*, in Chapter 3.3. As our goal is to build *algorithmic applications*, we provide a comprehensive discretization of the central quantities of the theory in Chapter 4.
Based on this framework, we develop ideas motivated by the successful application of the Laplace-Beltrami operator in Shape Analysis in Chapter 5 and Chapter 6 . Both chapters rely on the language and concepts introduced in the previous chapters. In Chapter 5 we discuss how the eigenvalue problem of the Dirac operator *changes under spin transformation*. In Chapter 6 we investigate *spectral geometric* ideas for the squared Dirac operator.
In Chapter 7, we directly address the problem of *specifying isometric deformations* in this framework of more general conformal deformations via an optimization based approach.
Finally, we close our investigation with a summary and concluding remarks in Chapter 8.
To provide the theoretical preliminaries for our discussion, we introduce some notions of classical Differential Geometry in the Appendix, a language that is used in particular in Chapter 6.3.
To ease the reading process, a nomenclature table is provided after the appendix.

This thesis would not exist without the help of others and I would like to thank those who provided me with scientific support and made my time at the chair interesting. In particular, I want to thank Dr. Emanuele Rodolà, Matthias Vestner and Mathieu Andreux for fruitful discussions and for getting me excited about the field of Shape Analysis. I am grateful to Prof. Dr. Daniel Cremers for giving me the opportunity to write my thesis at his chair and for constantly keeping up a visionary flair in the various research areas being tackled in the group. Their effort made my thesis time particularly valuable.

Thomas Frerix
Munich, November 2014

Contents

Chapter 1
Introduction

1.1 Classification of Shape Analysis

Within the last decade, the field of 3D *Shape Analysis* has undergone an explosive development. The evolution of the field has been catalyzed by two ambitious projects in engineering: 3D scanning and 3D printing. Whereas the former development enables economic and continuously better 3D models of the world around us, the latter development reverses this process, namely it generates physical objects from 3D data. In between lies the field of *Shape Analysis*: the *algorithmic* processing, evaluation and utilization of 3D data. Classical tasks in the field of *Shape Analysis* are the characterization of shape similarities and the computation of correspondences between shapes.

In order to arrive at the algorithmic aspect of *Shape Analysis*, a continuous mathematical description of three-dimensional objects has to be discretized and subsequently formulated in feasible algorithms. The point of view we choose in this thesis is that of *Differential Geometry*[1]. The overall goal of this approach is to properly discretize Continuous Differential Geometry (CDG) to arrive at a framework of Discrete Differential Geometry (DDG), for which a suitable algorithmic formulation is sought.

Along this pipeline, the number of *additional* aspects that have to be taken into account increases and therefore is adequately represented by a pyramid as shown in Fig. 1.1.
In the process of discretizing a continuous theory, the discrete objects should exhibit the key features of the continuous ones, in particular should converge to the continuous theory in a suitable sense. However, it is often not possible to recover *all* properties of, for example, an operator of the continuous theory. Consequently, a challenging research problem emerges on the level of DDG: finding the most suitable discretization for a given context. A prominent instance of this procedure is the Laplace-Beltrami operator ([27]).
Analogously, the algorithmic formulation of a discrete theory is far from canonical. In fact, the modeling process often leads to an optimization problem, for which it is as much an art as a skill to

[1] Another point of view is that of *Graph Theory*, which neglects the aspect of a continuous geometric theory and thus starting with a subsampled mesh offers and alternative paradigm at the level of a discrete theory.

find a feasible formulation. More precisely, problems arising in *Shape Analysis* are often quadratic or even combinatorial in their nature (cf. [21], [17]) and it is a challenge to find a *scalable* and *robust* algorithmic formulation.

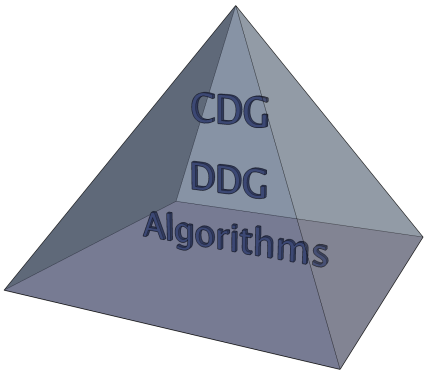

Figure 1.1: Classification of the field of *Shape Analysis*. As a number of additional aspects increases from Continuous Differential Geometry (CDG) over Discrete Differential Geometry (DDG) to an algorithmic formulation, this process can be represented by a pyramid.

This thesis touches several aspects of the paradigm pyramid Fig. 1.1. It serves as a lucid example of the problem hierarchy towards the bottom of the pyramid in highlighting the accumulation of posed problems. The choice for the theoretical framework of this thesis is rooted in classical Differential Geometry and is therefore underlined by a theoretical justification from the pyramid top.
Consequently, the point of view taken in this thesis may be classified as a *top-down* approach.

1.2 A top-down approach to Shape Analysis

At the heart of any application involving 3D shapes lies the geometric characterization of a surface. As a consequence, prior to being able to manipulate shapes, the question of a comprehensive and at best unique surface description has to be tackled. Within classical Differential Geometry, the Fundamental Theorem of Surface Theory due to Bonnet answers this question. In prose, it can be stated as follows:

Theorem 1.1 ([8])**.** *The first and second fundamental form determine a surface up to rigid Euclidean motion (rotation and translation).*

Important for understanding the geometry of surfaces[2] is the distinction between the abstract surface (M, g) and its (in general non-unique) immersion into $\mathbb{R}^3$. Geometrical quantities of the surface can be categorized as being intrinsic, that is, being fully determined by the metric g, and being extrinsic, that is, depending on the particular immersion. With the language of Theorem 1.1 this can be stated as follows: The first fundamental form completely determines the intrinsic geometry of a surface, whereas the second fundamental form also carries information about its immersion. Together, they uniquely define the outer appearance of a surface in ambient space, which we will call the *shape* of a surface.

As a consequence, the inverse problem arises naturally: can one prescribe two arbitrary quadratic forms as first and second fundamental form to obtain an immersed surface $f : M \to \mathbb{R}^3$ unique up to rigid motion? The answer is negative, which becomes evident by considering a moving frame surface description in the basis $\{f_{x_1}, f_{x_2}, N\}$ with local coordinates (x_1, x_2), outward normal field N and partial derivatives f_{x_1}, f_{x_2}: As the immersion is a smooth function, Schwarz' theorem states that second order derivatives exchange, $(f_{x_1})_{x_2} = (f_{x_2})_{x_1}$. This leads to compatibility restrictions for the two forms, called *integrability conditions*, which carry the names of Gauß, Mainardi and Codazzi ([8]):

$$\begin{aligned} l_{x_2} - m_{x_1} &= l\Gamma^1_{12} + m(\Gamma^2_{12} - \Gamma^1_{11}) - n\Gamma^2_{11} \\ m_{x_2} - n_{x_1} &= l\Gamma^1_{22} + m(\Gamma^2_{22} - \Gamma^1_{12}) - n\Gamma^1_{12}\,, \end{aligned} \tag{1.1}$$

where l, m, n are the coefficients of the local matrix representation of the second fundamental form and Γ^k_{ij} are the Christoffel symbols, which depend only on the first fundamental form and are *functions* of the local coordinates. Therefore, only forms satisfying Eq. (1.1) can be prescribed as first and second fundamental form.

As a coupled system of partial differential equations with *variable* coefficients Γ^k_{ij}, these equations are in general difficult to solve.

The theory of classical Differential Geometry has two features that hint at why the integrability conditions are expressed by such difficult equations: it is a theory in *local coordinates* and it imposes no restriction on the *class* of possible immersions. In particular immersions related by a

[2] We give an introduction to the classical Differential Geometry of surfaces in the Appendix.

diffeomorphism are covered by the theory.

Remark 1.2. These observations lead to conclude that any theory of Shape Analysis that aims to capture the intrinsic *and* extrinsic geometry of a surface, has to provide a mathematical formulation, within which the integrability conditions become manageable to solve. Phrased differently, such a formalism has to admit a feasible representation of a suitable shape space.

This thesis uses the formalism of a *quaternionic* surface description, which admits a formalization of shape space under the restriction of *conformally equivalent* surfaces. In particular, the formalism naturally incorporates *intrinsic* and *extrinsic* geometry. At an abstract level, it allows a formulation in the language of quaternion-valued differential forms and therefore admits a *coordinate free* surface description.

The theoretical foundations have been investigated in the late 90s and have been summarized in [13]. First applications have been recently realized in [4] for geometry processing tasks. These two works, in particular the latter one, are the main sources of inspiration for this thesis.

In contrast to the geometry processing applications developed in [4], we explore the Quaternionic Shape Analysis framework for the special case of *physical deformations* of *physical objects*. Whereas conformal deformations are the desired transformations for geometry processing tasks, as they preserve *texture* ([6]), physical surfaces are limited in local scaling and shearing. The associated class of deformations is that of *intrinsic isometries*. In fact, the class of conformal deformations is far too general and not discriminative enough for the analysis of isometric shapes. As a classical example, every simply connected surface is conformally equivalent to the sphere.
Fig. 1.2 shows possible deformation classes with allowed *local* transformations. For discrete surfaces, this corresponds to deformations of each triangle of the mesh. The table is ordered from left to right by inclusion.

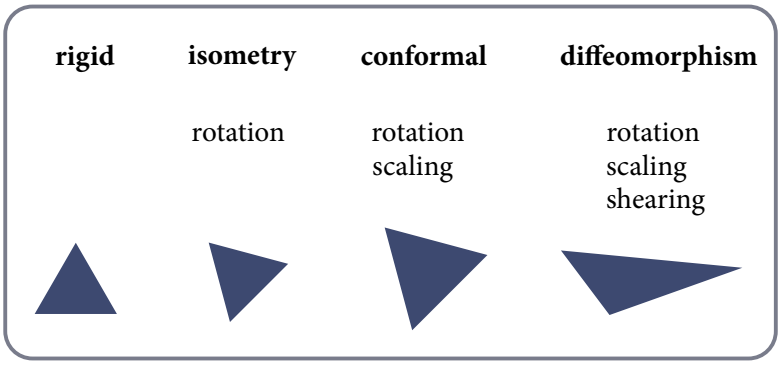

Figure 1.2: Transformation classes with possible local deformations. In the discrete case, these correspond to operations on the triangles of the mesh.

On the other hand, as outlined above, a surface is not uniquely described by the intrinsic geometry, but the extrinsic geometry has to be taken into account. In fact, as physical objects generally consist of large *rigid parts*, there are extrinsic quantities, such as mean curvature, that remain locally invariant under physical deformations. This effect is demonstrated in Fig. 1.3 and Fig. 1.4, which exhibit the TOSCA ([3]) dataset's cat in two (nearly) isometric poses, where the mean curvature of the shapes is displayed as a scalar function over the surface[3]. The mean curvature of large parts of the cat's body remains relatively constant on the overall scale of mean curvature change. Note that extreme values of mean curvature coincide with highly convex (positive mean curvature) and highly concave (negative mean curvature) regions. A significant change in mean curvature can be detected at articulated body parts, namely the joints of the movement. To visually highlight this effect, the change of mean curvature when going from the null-pose in Fig. 1.3 to the articulated motion in Fig. 1.4 is demonstrated in Fig. 1.5 on the null-pose.
Consequently, and in contrast to classical intrinsic descriptor methods[4], it is appealing to incorporate *extrinsic* geometrical features in the analysis of physical deformations.

In summary, the contribution of this thesis may be formulated as follows:

An exploration of Quaternionic Shape Analysis, incorporating intrinsic and extrinsic geometry, for the analysis of physical deformations.

[3] To correct for locally extremal values of mean curvature that distort the global scale, the 95th percentile of the data is displayed.

[4] most notably those based on Laplace-Beltrami diffusion geometry

Figure 1.3: Mean curvature of the TOSCA dataset's cat in null-pose on a linear scale from −0.9 (blue) over 0.0 (grey) to 0.9 (red) to highlight extreme values.

Figure 1.4: Mean curvature of the TOSCA dataset's cat in an articulated pose on a linear scale from −0.9 (blue) over 0.0 (gray) to 0.9 (red) to highlight extreme values.

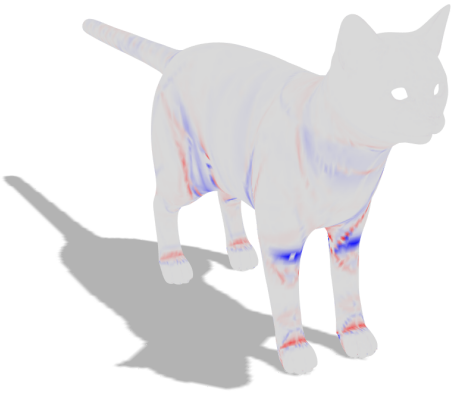

Figure 1.5: Difference in mean curvature when going from the null-pose of Fig. 1.3 to the articulated pose in Fig. 1.4 on a linear scale from −0.9 (blue) over 0.0 (gray) to 0.9 (red) to highlight extreme values. The difference is largest at the joints of the movement, whereas mean curvature remains almost invariant at the rigid parts.

Chapter 2

Quaternionic surface description

As outlined in the previous chapter, we are seeking a concise formulation of conformal deformations. As illustrated in Fig. 1.2, the possible local deformations are *rotation* and *scaling*. It turns out that quaternions are a natural language to describe exactly those two operations and provide the backbone for formalizing the class of conformal deformations.

2.1 Quaternions

The quaternion skew-field $\mathbb{H}$ is a four-dimensional real vector space with basis $\{\mathbf{1}, \mathrm{i}, \mathrm{j}, \mathrm{k}\}$ satisfying the algebraic relations

$$\mathrm{i}^2 = \mathrm{j}^2 = \mathrm{k}^2 = \mathrm{ijk} = -\mathbf{1}. \tag{2.1}$$

A quaternion $q = (a, b, c, d) \in \mathbb{H}$ can be formally divided into a real and an imaginary part as

$$\begin{aligned} \mathrm{Re}(q) &= a \\ \mathrm{Im}(q) &= b\mathrm{i} + c\mathrm{j} + d\mathrm{k}. \end{aligned} \tag{2.2}$$

Using the identification $\mathrm{Re}(\mathbb{H}) \cong \mathbb{R}$, $\mathrm{Im}(\mathbb{H}) \cong \mathbb{R}^3$, a quaternion can be written as

$$q = q^{(s)} + q^{(v)}, \tag{2.3}$$

where $q^{(s)} \in \mathrm{Re}(\mathbb{H})$ is the scalar part ($\cong$ real part) and $q^{(v)} \in \mathrm{Im}(\mathbb{H})$ is the vector part ($\cong$ imaginary part). The algebraic relations (2.1) uniquely determine an associative, non-commutative product, the *Hamilton product*, which in vector calculus language can be expressed as

$$qp = \underbrace{q^{(s)}p^{(s)} - \left\langle q^{(v)}, p^{(v)} \right\rangle_{\mathbb{R}^3}}_{\text{real part}} + \underbrace{q^{(s)}p^{(v)} + p^{(s)}q^{(v)} + q^{(v)} \times p^{(v)}}_{\text{imaginary part}}. \tag{2.4}$$

As in the remainder of this thesis, we use a notation that will always be clear from context: when identifying $\mathbb{H} \cong \mathbb{R}^4$, $\mathrm{Re}(\mathbb{H}) \cong \mathbb{R}$, $\mathrm{Im}(\mathbb{H}) \cong \mathbb{R}^3$, we will *not change the typographic symbol*. Cross and scalar products for purely imaginary quaternions are meant as for the vectors in $\mathbb{R}^3$, whereas

the result of such a vector operation may be identified with a real or imaginary quaternion and may be added to another quaternion. Furthermore, every quaternion product that is not designated by a specific operator is the general Hamilton product Eq. (2.4) of two quaternions.

Expression Eq. (2.4) contains two fundamental geometric products in Euclidean space, the scalar product and the cross product. In particular, for $p, q \in \mathrm{Im}(\mathbb{H})$ we recover

$$qp = q \times p - \langle q, p \rangle_{\mathbb{R}^3} . \tag{2.5}$$

Conjugation is defined as

$$\overline{q} = q^{(s)} - q^{(v)}, \tag{2.6}$$

where

$$\overline{qp} = \overline{p}\overline{q}, \tag{2.7}$$

and the norm of a quaternion is given by

$$|q|^2 = \overline{q}q. \tag{2.8}$$

It follows that the inverse of a quaternion q is

$$q^{-1} = \frac{\overline{q}}{|q|^2}. \tag{2.9}$$

A special role play unit quaternions with $|q| = 1$, as their similarity transformation on $x \in \mathrm{Im}(\mathbb{H})$ corresponds to a *rotation* in $\mathbb{R}^3$, which is illustrated in Fig. 2.1. If $q = \cos(\theta/2) - \sin(\theta/2)u$ for some rotation axis $u \in \mathrm{Im}(\mathbb{H})$ and $\theta \in [0, 2\pi)$, then the map $x \mapsto \overline{q}xq$ realizes a rotation around u by an angle θ. If, more generally, $|q| \neq 1$, then the similarity transformation results in *rotation* induced by $q/|q|$ and *scaling* by $|q|^2$.

Since for $q = q^{(s)} + q^{(v)}$, the vector part can be locally decomposed in the frame basis $\{f_{x_1}, f_{x_2}, N\}$ of a conformal immersion $f : M \to \mathbb{R}^3$ with differential df, surface normal field N and local coordinates (x_1, x_2), any quaternion-valued function $\psi : M \to \mathbb{H}$ can be decomposed as

$$\psi = a + df(Y) + bN, \tag{2.10}$$

for the surface normal field N, some vector field Y on M and real valued functions $a, b : M \to \mathbb{R}$.

As the Gauss map N appears in this decomposition, it also encodes *extrinsic* geometry. More precisely, whereas Eq. (2.3) is a decomposition based on the quaternion structure only, decomposition (2.10) is *f-dependent*.

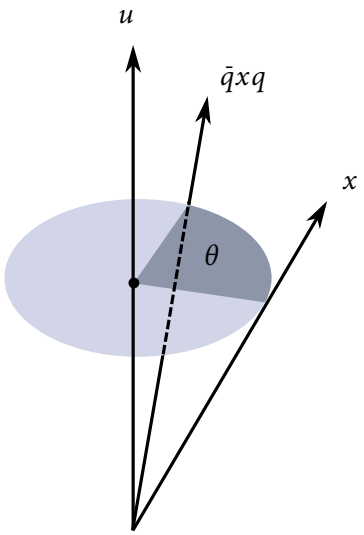

Figure 2.1: Illustration of a rotation induced by a quaternion similarity transformation of vector $x \in \mathrm{Im}(\mathbb{H})$ around an axis $u \in \mathbb{R}^3$ by an angle $\theta \in [0, 2\pi)$.

As an example, consider a topological surface M that admits two different immersions

$$f_1 : M \to S_1 \subset \mathbb{R}^3$$
$$f_2 : M \to S_2 \subset \mathbb{R}^3 ,$$

that is, they differ in their extrinsic geometry, but posses the same metric properties. Take a quaternion-valued function $\psi : M \to \mathbb{H}$, $p \mapsto N_{S_1}$, which has vanishing real part and whose vector part equals that of the Gauss map of the surface S_1. The function ψ then admits the decompositions

$$\psi = N_{S_1}$$
$$\psi = df_2(Y) + bN_{S_2} ,$$

which is the same *quaternionic* function, but as the immersions differ, so does the decomposition.

2.2 Differential forms

A concise and coordinate free language[5] to express ideas of Differential Geometry is that of Exterior Calculus. The main objects are (differential) forms[6], which are quaternion-valued in this thesis. The important operators are the wedge product $\wedge$, the Hodge star operator $\star$ and the exterior derivative d.
We will develop an intuitive approach starting from real differential forms in the Euclidean case, over real differential forms in the surface case, up to the quaternionic surface case. This language

[5] An example where this is helpful for a concise computation is in the proof of Theorem 5.1.
[6] All forms appearing in this thesis are *differential* forms even if not written explicitly.

of quaternion-valued differential forms over surfaces will be the basis to express the ideas pursued in Chapter 5 and Chapter 6. Even though not all technical details outlined in this chapter will be used explicitly later on, they should serve as basis to deal with general calculations of quaternionic differential forms.

2.2.1 Real valued forms on Euclidean space

A *1-form* ω over the Euclidean plane $\mathbb{R}^2$ is a real linear function $\omega : \mathbb{R}^2 \to \mathbb{R}$, i.e. for $w_1, w_2 \in \mathbb{R}^2$, $a, b, \in \mathbb{R}$,

$$\omega(aw_1 + bw_2) = a\omega(w_1) + b\omega(w_2).$$

ω can be thought of to be in the *dual space* of $\mathbb{R}^2$. We can obtain an intuitive understanding of such a 1-form as follows. Take two vectors $v, w \in \mathbb{R}^2$. Then a 1-form ω associated with w can be interpreted as

$$\omega(v) = \langle w, v \rangle_{\mathbb{R}^2}, \tag{2.11}$$

namely the *orthogonal projection* from v onto w as illustrated in Fig. 2.2. In fact, the correspondence – or *duality* – between w and ω should not be surprising, as it is a manifestation of the self-duality property of $\mathbb{R}^n$: there is a one-to-one correspondence between linear functionals and the vector space elements themselves.

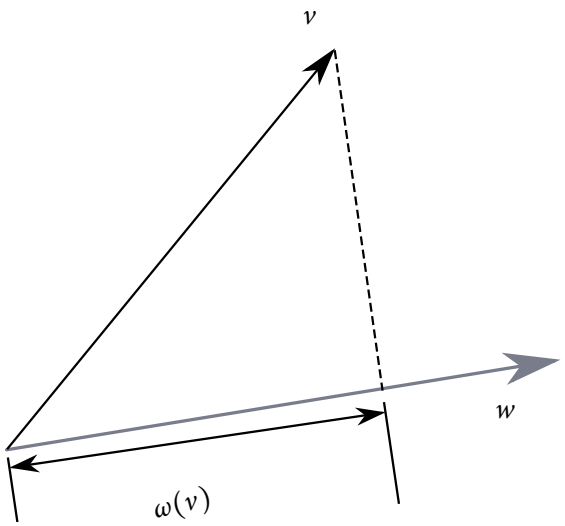

Figure 2.2: Illustration of 1-forms on $\mathbb{R}^2$. The real number $\omega(v)$ is the projected length from v onto w.

Just as with vectors, the space of 1-forms can be constructed from a basis. Denote the basis of $\mathbb{R}^2$ by $\{\frac{\partial}{\partial x^1}, \frac{\partial}{\partial x^2}\}$, such that[7]

$$v = v^1 \frac{\partial}{\partial x^1} + v^2 \frac{\partial}{\partial x^2}.$$

[7] With this notation, we already have tangent planes of a surface in mind.

We denote the basis of the dual space to $\mathbb{R}^2$ as $\{dx^1, dx^2\}$, which is constructed by the *dual relation*

$$dx^i\left(\frac{\partial}{\partial x^j}\right) = \delta^i_j = \begin{cases} 1 & \text{if } i = j \\ 0 & \text{otherwise} \end{cases}$$

The choice to use lower and upper indices underlines the dual character.

To introduce the wedge product and the Hodge star operator, it is illustrative to consider 2-forms in $\mathbb{R}^3$, which is a natural step from the example above.

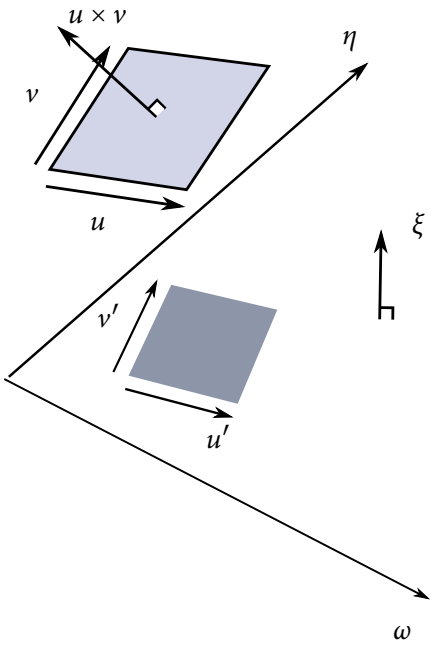

Figure 2.3: Illustration of 2-forms on $\mathbb{R}^3$. The real number $\omega \wedge \eta(u, v)$ is the projected area of $u \times v$ onto the plane spanned by (ω, η).

Take two vectors $u, v \in \mathbb{R}^3$ that form a parallelogram and two 1-forms ω, η over $\mathbb{R}^3$ that can be thought of as vectors[8] spanning a plane as depicted in Fig. 2.3. If we project u and v onto ω and η, respectively, then we obtain vectors u', v' in the plane spanned by ω and η as

$$\begin{aligned} u' &= (\omega(u), \eta(u)) \\ v' &= (\omega(v), \eta(v)) \,. \end{aligned}$$

The signed projected area is given by the cross product[9]

$$u' \times v' = \omega(u)\eta(v) - \omega(v)\eta(u).$$

[8] We use the same notation for the dual objects ω as a 1-form and as a vector.
[9] The third vector component is set to zero.

This procedure is an illustration of the *wedge product* between 1-forms, which we can now define as exactly this expression

$$\omega \wedge \eta(u, v) := \omega(u)\eta(v) - \omega(v)\eta(u). \tag{2.12}$$

$\omega \wedge \eta$ is the generic example of a 2-form, as most 2-forms in this thesis are constructed from two 1-forms via the wedge product. Note that the 2-form $\omega \wedge \eta$ takes *two* vectors as an argument[10]. Even though the wedge product was derived from a special illustrative case, this definition is a general one.
The wedge product in Eq. (2.12) behaves *antisymmetric*,

$$\omega \wedge \eta = -\eta \wedge \omega.$$

From this property it directly follows that the wedge product of a 1-form with itself has to be zero, since

$$\omega \wedge \omega = -\omega \wedge \omega\,.$$

So far we have been discussing 1- and 2-forms, but omitted 0-forms. The reason is that there is no new concept for 0-forms, they are just *smooth functions* on M. The wedge product between a 0-form ϕ and a 1-form ω is the pointwise product of the function with the 1-form,

$$\phi \wedge \omega = \phi\omega\,. \tag{2.13}$$

Analogously, this holds for the wedge product of a 0-form ϕ and a 2-form $\omega \wedge \eta$,

$$\phi(\omega \wedge \eta) = \phi\omega \wedge \eta = \omega \wedge \phi\eta\,. \tag{2.14}$$

To conclude, for real 1-forms η, ω, ξ, the wedge product has the following properties.

- **Antisymmetry:** $\omega \wedge \eta = -\eta \wedge \omega$
- **Associativity:** $\omega \wedge (\eta \wedge \xi) = (\omega \wedge \eta) \wedge \xi$
- **Distributivity:** $\omega \wedge (\eta + \xi) = \omega \wedge \eta + \omega \wedge \xi$

The illustration in Fig. 2.3 is at the heart of *Hodge duality*. One can compare the alignment of the parallelogram spanned by (u, v) with the plane (ω, η) either by calculating its projected area *or* by determining how well the normal $u \times v$ aligns with the normal ξ of the plane (ω, η). In the language of differential forms,

$$\xi(u \times v) = \omega \wedge \eta(u, v)\,, \tag{2.15}$$

[10] This generalizes to k-forms, which take k vectors as an argument.

where ξ is a 1-form evaluated on the vector $u \times v$.
Stated equivalently, in three-dimensional space, the same geometric objects can be related by either considering two dimensions or the one remaining dimension.

More generally, in n-space, we can use k dimensions to describe a geometric object or the remaining $(n-k)$-dimensions. We formally introduce the Hodge star operator, which switches between those two points of view, together with differential forms on surfaces.

2.2.2 Real valued forms on surfaces

Let (M, g) be a two-dimensional surface immersed into $\mathbb{R}^3$ via an immersion $f : M \to \mathbb{R}^3$. We will henceforth use the vector field notation, that is, for $X \in TM$, we write the evaluation of a 1-form ω as $\omega(X)$, which implies a pointwise evaluation on vectors as $\omega_p(X_p),\ \forall p \in M$.

Definition 2.1. *A* k-form ω *on* M, $k \in \{1, 2\}$, *is a real linear function* $\omega : \bigwedge_{l=1}^{k} TM \to \mathbb{R}$.

In this definition, $\bigwedge_{l=1}^{k} TM$ denotes the exterior algebra over the tangent bundle TM. Phrased differently, a k-form is in the dual space to $\bigwedge_{l=1}^{k} TM$, which we denote by $\Omega_k(M) := \left(\bigwedge_{l=1}^{k} TM\right)^*$. We will not discuss details of the notation or the concept of an exterior algebra, as it leaves the scope of this thesis and will not be used henceforth. However, we want to emphasize the one important implication of this notation for the low dimensional cases under consideration. For the case $k = 1$, the space $\bigwedge^1 TM$ is just TM itself and for the case $k = 2$, $\bigwedge^2 TM$ does not imply more than a sign change under permutation, i.e. for $(X, Y) \in TM \wedge TM$, $(Y, X) = -(X, Y)$. This sign change can be recognized as a property of the cross product in Eq. (2.15). Thus the notation $\bigwedge_{l=1}^{k} TM$ encodes the antisymmetry of differential forms that we have already discovered and which is not mentioned explicitly in Def. 2.1.

Since the tangent space of the surface M is two-dimensional, it is a canonical step from the Euclidean plane $\mathbb{R}^2$. The input arguments of the forms are now *tangent vectors*.
In local coordinates (x_1, x_2) around a point $p \in M$, we denote the basis of the tangent plane at p by $\{\frac{\partial}{\partial x^1}, \frac{\partial}{\partial x^2}\}$. The corresponding dual basis is $\{dx^1, dx^2\}$.

Resuming the Hodge duality discussion, we define the Hodge star operator acting on a k-form $\omega \in \Omega_k(M)$ as the operator ([9])

$$\star : \Omega_k(M) \to \Omega_{2-k}(M) \qquad k \in \{0, 1, 2\}\,, \tag{2.16}$$

that satisfies

$$\eta \wedge \star\omega = \langle \eta, \omega \rangle\, \sigma \qquad \forall \eta \in \Omega_k(M)\,, \tag{2.17}$$

where $\langle \cdot, \cdot \rangle$ is the inner product on $\Omega_k(M)$ and σ is the volume form, which can be expressed in local coordinates as $\sigma = dx^1 \wedge dx^2$. Thus the Hodge star operator $\star$ transforms a k-form into a $(2-k)$-form. To specify the inner product on $\Omega_k(M)$, let us take a concrete basis expansion in local coordinates. An element $\omega \in \Omega_k(M)$ can be expressed as

$$\omega = \begin{cases} \omega_0 & \text{if } k = 0 \\ \omega_1 dx^1 + \omega_2 dx^2 & \text{if } k = 1 \\ \omega_3 (dx^1 \wedge dx^2) & \text{if } k = 2\,. \end{cases}$$

Then an inner product between $\omega, \eta \in \Omega_k(M)$ is given by $\langle \omega, \eta \rangle = \sum_j \omega_j \eta_j$.

With this definition at hand, we can describe the action of the Hodge star operator on the basis elements. Let us start with the basis elements of 1-forms in local coordinates.
For an arbitrary 1-form ω,

$$\begin{aligned} \omega \wedge \star dx^1 &\stackrel{!}{=} \left\langle \omega, dx^1 \right\rangle dx^1 \wedge dx^2 \\ &= \left\langle \omega_1 dx^1 + \omega_2 dx^2, dx^1 \right\rangle dx^1 \wedge dx^2 \\ &= \omega_1 dx^1 \wedge dx^2. \end{aligned} \tag{2.18}$$

Further,

$$\begin{aligned} \omega \wedge \star dx^1 &= (\omega_1 dx^1 + \omega_2 dx^2) \wedge \star dx^1 \\ &= \omega_1 dx^1 \wedge \star dx^1 + \omega_2 dx^2 \wedge \star dx^1. \end{aligned}$$

Comparing these two expressions, it follows that $\star dx^1 = dx^2$. An analogous calculation yields $\star dx^2 = -dx^1$.
The action of the Hodge star operator on the 2-form basis $dx^1 \wedge dx^2$ and on the 0-forms identically equal to 1, denoted as $\mathbf{1}$, follow directly from the definition Eq. (2.17):

$$\begin{aligned} \star \mathbf{1} &= dx^1 \wedge dx^2 \\ \star (dx^1 \wedge dx^2) &= \mathbf{1} \end{aligned}$$

Altogether, we arrive at the following conclusion, which summarizes the important facts for calculations involving the Hodge star operator in practice.

Conclusion on the Hodge star operator in the surface case

The Hodge star operator acts on the basis elements of local coordinates as

$$\begin{aligned} \star\mathbf{1} &= dx^1 \wedge dx^2 \\ \star(dx^1 \wedge dx^2) &= \mathbf{1} \\ \star dx^1 &= dx^2 \\ \star dx^2 &= -dx^1 \end{aligned} \tag{2.19}$$

We deduce that the Hodge star acts on the 1-form basis as a *counterclockwise* 90° *rotation*. As a consequence, the action of the Hodge star operator on the forms appearing in the surface case is:

0-forms Let ϕ be an $\mathbb{R}$-valued 0-form on M, σ the volume form, then

$$\star\,\phi = \sigma\phi. \tag{2.20}$$

1-forms Let ω be an $\mathbb{R}$-valued 1-form on M, $\mathcal{J}$ the complex structure introduced in the Appendix, namely a counterclockwise 90° rotation, then

$$(\star\omega)(X) = \omega(\mathcal{J}X)\ \forall X \in TM\,. \tag{2.21}$$

2-forms Let η be an $\mathbb{R}$-valued 2-form on M, σ the volume form, then

$$(\star\eta)\sigma = \eta\,. \tag{2.22}$$

It follows that every 2-form η is a rescaled version of the volume form by the 0-form $\star\eta := \eta(X, \mathcal{J}X)$, for any vector field $X \in TM$ with $|df(X)| = 1$. Note that if we fix such a $X \in TM$, then $\eta(X, \mathcal{J}X)$ is a *function* on M, that is, $\eta(X, \mathcal{J}X) : M \to \mathbb{R}, p \mapsto \eta(X_p, (\mathcal{J}X)_p)$.

Furthermore, for an $\mathbb{R}$-valued 0-forms ϕ, ψ, and k-forms ω, η ($k \in \{0, 1, 2\}$) on a surface M immersed into $\mathbb{R}^3$ the following identities hold for the Hodge star operator[11]:

$$\begin{aligned} \star(\phi\omega + \psi\eta) &= \phi(\star\omega) + \psi(\star\eta) \\ \star\star\,\omega &= (-1)^{k(2-k)}\omega \\ \langle\star\omega, \star\eta\rangle &= \langle\omega, \eta\rangle\ . \end{aligned} \tag{2.23}$$

[11] A discussion of the structural properties of the Hodge star operator is given in [9].

The *exterior derivative* $d : \Omega_k(M) \to \Omega_{k+1}(M)$ is the unique $\mathbb{R}$-linear mapping from k-forms to $(k+1)$-forms that satisfies ([10])

1. $d\phi$ is the differential of ϕ for any smooth function $\phi \in \Omega_0(M)$
2. $d(d\omega) = 0 \quad \forall \omega \in \Omega_k(M)$
3. $d(\omega \wedge \eta) = d\omega \wedge \eta + (-1)^{\deg \omega}(\omega \wedge d\eta) \quad \forall \omega, \eta : \omega \wedge \eta \in \Omega_k(M)$

The third property is called the *Leibniz rule* and includes as a special case the product rule for the differentiation of functions. A k-form ω is called *closed* if $d\omega = 0$. It is called *exact* if $\omega = d\eta$ for some $\eta \in \Omega_{k-1}(M)$. As $d(d\omega) = 0$, every exact from is closed.
By linearity and the Leibniz rule, the exterior derivative is conveniently applied to the basis elements as the following example of a 1-form $\omega = \omega_1 dx^1 + \omega_2 dx^2$ demonstrates.
Due to linearity,

$$d\omega = d(\omega_1 dx^1) + d(\omega_2 dx^2) + d(\omega_3 dx^3)\,. \tag{2.24}$$

By the Leibniz rule, each term of Eq. (2.24) can be written as

$$d(\omega_i dx^i) = d\omega_i \wedge dx^i + \omega_i \wedge ddx^i = \sum_{j=1}^{2} \frac{\partial \omega_i}{\partial x^j} dx^j \wedge dx^i\,,$$

as $ddx^i = 0$.

The language of differential forms allows a concise formulation of *surface integration*. A powerful theorem that is used in the thesis for the discretization via the Finite Element paradigm is *Stoke's theorem*,

$$\int_\Omega d\omega = \int_{\partial\Omega} \omega \tag{2.25}$$

for a domain $\Omega \subset M$ and a differential form ω on M.

2.2.3 Quaternion-valued forms on surfaces

In the quaternionic case, we unfortunately do not have the intuitive examples as for real valued forms at hand. However, the abstract operations of Exterior Calculus form a powerful language, which we will use in the remainder of the thesis. In the following, we will outline how the *non*-commutativity of quaternions affects these properties, which will lead to a set of rules that we need for calculations carried out later on in this thesis.
Whereas generic real valued differential forms are denoted by ω, η, generic quaternion-valued differential forms will be denoted by α, β to always be aware that we are dealing with non-commutative objects.

Note that as surfaces are intrinsically 2-dimensional, the quaternionic forms appearing in this framework are

- **0-forms**: smooth $\mathbb{H}$-valued functions on M
- **1-forms**: real-linear maps that take a vector field on M to an $\mathbb{H}$-valued function
- **2-forms**: maps that take two vector fields on M to an $\mathbb{H}$-valued function

As in the commutative case, quaternionic differential 1-forms are *real linear*, which means that for any real valued function φ and vector fields X, Y,

$$\alpha(\varphi X + Y) = \varphi\alpha(X) + \alpha(Y). \tag{2.26}$$

For 1-forms α, β, the quaternionic wedge product is defined as

$$\alpha \wedge \beta(X, Y) := \alpha(X)\beta(Y) - \alpha(Y)\beta(X), \tag{2.27}$$

where all products appearing are quaternionic Hamilton products, as defined in Eq. (2.4).
With a 0-form h, the following identities will be useful in calculations ([13]):

$$\begin{aligned} \overline{\alpha \wedge \beta} &= -\overline{\beta} \wedge \overline{\alpha}, \\ \alpha \wedge h\beta &= \alpha h \wedge \beta, \\ h\alpha \wedge \beta &= h(\alpha \wedge \beta). \end{aligned} \tag{2.28}$$

In addition, if φ is a real valued function, then

$$\alpha \wedge \varphi\beta = \varphi(\alpha \wedge \beta), \tag{2.29}$$

which would *not* be true if φ was a general quaternion-valued function.
As relations (2.28) show, it is in general also *not* true that $\alpha \wedge \beta = -\beta \wedge \alpha$.
The usual Leibniz rule on the other hand remains valid,

$$d(\alpha \wedge \beta) = d\alpha \wedge \beta + (-1)^{\deg(\alpha)}(\alpha \wedge d\beta), \tag{2.30}$$

where the degree of a k-form is k. The properties for the Hodge star operator derived in the last section remain valid as well.

Convention for 2-forms If not indicated otherwise, a 2-form $\alpha \wedge \beta$ will always be evaluated at a *single* vector field defined by

$$(\alpha \wedge \beta)(X) := \alpha \wedge \beta(X, \mathcal{J}X) \tag{2.31}$$

Phrased differently, a 2-form will be identified with the associated quadratic form.
A central expression is that of a *volume*[12], which is measured by the volume form σ,

$$\sigma = \frac{1}{2} df \wedge Ndf. \tag{2.32}$$

With the convention (2.31) in mind, the wedge product Eq. (2.27) can be written as

$$\alpha \wedge \beta = \alpha(\star\beta) - (\star\alpha)\beta. \tag{2.33}$$

In accordance with [4] and [13], we will denote the volume form of a conformal immersion as $|df|^2$, which, using $\star df = Ndf$ for a conformal immersion f, can be expressed as

$$|df|^2 = \frac{1}{2} df \wedge \star df. \tag{2.34}$$

To denote the Hodge star operator on 2-forms, we will often write the quotient of a 2-form η and the conformal volume form $|df|^2$, which we *define* as

$$\frac{\eta}{|df|^2} := \star\eta. \tag{2.35}$$

The reasoning behind this notation stems from Eq. (2.22).
As an example for the formalism introduced in this section, we derive an alternative expression for the volume form in concise notation. We use the convention (2.31) together with Eq. (2.33) as well as the relations listed as Eqs. (2.23) :

$$\begin{aligned}
|df|^2 &= \frac{1}{2}(df \wedge \star df) \\
&= \frac{1}{2}(df(\star\star df) - (\star df)(\star df)) \\
&= \frac{1}{2}(-dfdf - \underbrace{(\star df) \times (\star df)}_{=0} + \langle \star df, \star df \rangle) \\
&= \frac{1}{2}(-dfdf + \langle df, df \rangle) \\
&= \frac{1}{2}(-dfdf - (\underbrace{df \times df}_{=0} - \langle df, df \rangle)) \\
&= -dfdf,
\end{aligned} \tag{2.36}$$

where every appearing 1-form is evaluated at some fixed vector field $X \in TM$.

[12] The two-dimensional volume in this case is surface area.

2.3 Quaternionic inner product spaces

In order to have the apparatus of linear algebra available for the analysis of quaternionic matrices, following [11], we will introduce the concept of a *quaternionic inner product space*. As can be expected, difficulties arise due to the non-commutativity of quaternions. We choose to define $\mathbb{H}$-vector spaces and quaternionic inner product spaces with scalar multiplication from the right. Apart from this choice, the usual properties of spaces over regular fields hold. To be precise, we list the formal definitions of the spaces we are working with.

Definition 2.2. *An additive abelian group V is a* right $\mathbb{H}$-vector space *if there is a map $V \times \mathbb{H} \to V$, under which the image of each pair $(\lambda, q) \in V \times \mathbb{H}$ is denoted by λq, such that for all $q, q_1, q_2 \in \mathbb{H}$ and $\lambda, \lambda_1, \lambda_2 \in V$ it holds that*

$$\begin{aligned}(\lambda_1 + \lambda_2)q &= \lambda_1 q + \lambda_2 q\\ \lambda(q_1 + q_2) &= \lambda q_1 + \lambda q_2\\ \lambda(q_1 q_2) &= (\lambda q_1)q_2\\ \lambda\mathbf{1} &= \lambda\,.\end{aligned}$$

Definition 2.3. *A right $\mathbb{H}$-vector space V is a* quaternionic inner product space *if there is a map $\langle\cdot,\cdot\rangle : V \times V \to \mathbb{H}$ such that for all $q, q_1, q_2 \in H$ and $\lambda, \lambda_1, \lambda_2 \in V$ it holds that*

$$\begin{aligned}\langle\lambda, \lambda_1 + \lambda_2\rangle &= \langle\lambda, \lambda_1\rangle + \langle\lambda, \lambda_2\rangle\\ \langle\lambda_1, \lambda_2 q\rangle &= \langle\lambda_1, \lambda_2\rangle\, q\\ \langle\lambda_1, \lambda_2\rangle &= \overline{\langle\lambda_2, \lambda_1\rangle}\\ \langle\lambda, \lambda\rangle \geq 0 \text{ and } \langle\lambda, \lambda\rangle = 0 &\Leftrightarrow \lambda = 0\,.\end{aligned}$$

The example of a finite dimensional *quaternionic inner product space* that we will use throughout this thesis is $\mathbb{H}^n$. It is equipped with the quaternionic inner product

$$\langle\lambda, \mu\rangle_{\mathbb{H}^n} = \sum_{k=1}^{n} \overline{\lambda}_k \mu_k, \tag{2.37}$$

where the term-wise operation is the non-commutative Hamilton product as defined in Eq. (2.4).

The above theory extends to infinite dimensional quaternionic inner product spaces [25]. The example appearing in this thesis is the Hilbert space $L^2(M, \mathbb{H})$, the space of square integrable quaternionic functions on M, with the quaternionic inner product

$$\langle\phi, \psi\rangle_{L^2(M,\mathbb{H})} = \int_M \overline{\phi}\psi |df|^2. \tag{2.38}$$

2.4 The spectral theorem for quaternionic normal matrices

In order to conduct a spectral geometry of differential operators on quaternion-valued functions, as in Chapter 5 and Chapter 6, we would like to have an expansion of such functions in terms of a suitable basis related to the operator itself. As for matrices over $\mathbb{C}$, normal quaternion matrices are diagonalizable. Formally, this can be stated as

Theorem 2.4. *([11]) Assume that V is a n-dimensional quaternionic inner product space. Then an endomorphism $T : V \to V$ is normal if and only if there are $\mu_1, \ldots, \mu_n \in V$ and $\gamma_1, \ldots, \gamma_n \in \mathbb{C}^+$, the closed complex upper half plane, such that:*

1. $\{\mu_1, \ldots, \mu_n\}$ *is an $\mathbb{H}$-independent generating set for V*
2. $\langle \mu_k, \mu_l \rangle = \delta_{kl}$
3. $T\mu_k = \gamma_k \mu_k$
4. $T\lambda = \sum_{k=1}^{n} \gamma_k \mu_k \langle \mu_k, \lambda \rangle \quad \forall \lambda \in V$

More is true for hermitian quaternion matrices:

Theorem 2.5 ([11])**.** *If $Q \in \mathbb{H}^{n\times n}$ is hermitian, that is, $Q^\dagger = Q$, then every right eigenvalue of Q is real.*

This theory also extends to the case of normal operators on $L^2(M, \mathbb{H})$ ([25]), which we will use in discussions of the continuous theory.

It is worth pointing out a peculiarity of a quaternionic eigenvalue problem.

Theorem 2.6 ([11])**.** *Let $(q, \xi) \in \mathbb{H} \times \mathbb{H}^n$ be a right eigensolution for $Q \in \mathbb{H}^{n\times n}$, then $(w^{-1}qw, \xi w)$ is also a right eigensolution for Q for any non-zero $w \in \mathbb{H}$.*

The proof is a one-line calculation:

$$Q(\xi w) = (Q\xi)w = (\xi q)w = (\xi w)(w^{-1}qw). \tag{2.39}$$

According to this theorem, if Q is a hermitian quaternion matrix, then $q \in \mathbb{R}$ commutes with any non-zero $w \in \mathbb{H}$, from which follows

Corollary 2.7. *Let $(q, \xi) \in \mathbb{H} \times \mathbb{H}^n$ be a right eigensolution for $Q \in \mathbb{H}^{n\times n}$ with $Q^\dagger = Q$, then $(q, \xi w)$ is also a right eigensolution for Q for any non-zero $w \in \mathbb{H}$.*

Remark 2.8. As a geometric consequence, every eigensolution of a hermitian quaternion matrix is unique up to *global* rotation and scaling.

Chapter 3

Shape space, spin transformation and integrability

As outlined in Chapter 1.2, we are seeking a suitable representation of the shape space of conformal immersions. We introduce the coordinates in conformal shape space, *mean curvature half-densities*, in Chapter 3.1. As deformations within conformal shape space, we consider *spin transformations*, which we present in Chapter 3.2. Based on these concepts, we give the definition of conformal shape space in Chapter 3.4.

As outlined in the Appendix, *any* surface admits a conformal immersion $f : M \to \mathbb{R}^3$. Unfortunately, immersions $f : M \to \mathbb{R}^3$ are not well suited for this description as they do not form a vector space: the sum of two conformal immersions is not necessarily conformal. However, a conformal immersion is (almost)[13] uniquely determined by the metric and its *mean curvature half-density*, which does admit a vector space structure ([14]). A conformal shape space representation based on mean curvature half-densities is investigated in [4], which we will follow closely.

3.1 Half-densities

Let M be a topological surface with complex structure $\mathcal{J}$ and f an immersion such that

$$df(\mathcal{J}X) = N \times df(X) \quad \forall X \in TM\,,$$

that is, f is a conformal immersion[14]. A *half-density* is a (in general non-linear[15]) map

$$\varphi|df| : TM \to \mathbb{R}, X \mapsto \varphi|df(X)|\,,$$

[13] Exceptional cases are rather exotic and can be neglected for applications. They are characterized in [14] and termed *Bonnet pairs* therein.

[14] The action of $\mathcal{J}$ corresponds to a 90° counterclockwise rotation in tangent space.

[15] Therefore half-densities are not 1-forms.

for some real valued function φ in $L^2(M, \mathbb{H})$. This means that at a point $p \in M$, the vector X_p is mapped to its length in the ambient space $\mathbb{R}^3$ scaled by $\varphi(p)$.

These maps form a real vector space

$$\mathcal{H} := \left\{ \varphi |df| : TM \to \mathbb{R}, X \mapsto \varphi |df(X)| \,\middle|\, \varphi \in L^2(M, \mathbb{H}) \right\} \tag{3.1}$$

by defining

$$(\varphi_1 + \gamma\varphi_2)|df| := \varphi_1|df| + \gamma\varphi_2|df|\,, \tag{3.2}$$

with $\gamma \in \mathbb{R}$.

Moreover, the space of half-densities is a Hilbert space with the inner product

$$\langle \varphi_1|df|, \varphi_2|df| \rangle_{\mathcal{H}} := \int_M \varphi_2\varphi_2|df|^2 = \langle \varphi_1, \varphi_2 \rangle_{L^2(M,\mathbb{H})}\,. \tag{3.3}$$

In particular, there is a notion of orthogonality and thus of *direction* on $\mathcal{H}$.

Altogether, this means that for a fixed immersion f, $\mathcal{H}$ inherits the vector space structure from $L^2(M, \mathbb{H})$.

As a special case, taking $\varphi = H$, the mean curvature of the immersion of the surface M, we obtain the *mean curvature half-density* $\mu := H|df| \in \mathcal{H}$. Because of the inner product space structure of $\mathcal{H}$, it is possible to conduct a calculus of mean curvature half-densities, which leads to the definition in conformal shape space in Chapter 3.4. Mean curvature half-densities can be regarded as coordinates in this shape space.

Besides the structural advantage there are two more aspects, which make mean curvature half-density attractive for Shape Analysis and superior to mean curvature by itself.

First, since $H \sim 1/|df|$, μ is scale-invariant, meaning that a shape representation does not depend on the global scale of the immersion, which is a desired property from a computational point of view.

Secondly, because of this scaling behavior, mean curvature itself is not a good descriptor for global *shape appearance* as an increase (decrease) in mean curvature can be caused by decreasing (increasing) the local scale *or* by positive (negative) bending of the shape. Consider the comparison of a sphere and an ellipsoid for mean curvature and mean curvature half-density in Fig. 3.1 and Fig. 3.2. Both figures show deformations of the unit sphere. In Fig. 3.1a and Fig. 3.2a, the radius is reduced to half of its length, in Fig. 3.1b and Fig. 3.2b the x-axis is doubled in length, whereas y- and z-axis remain at unit length. The bended sides of the ellipsoid in Fig. 3.1b and the sphere in Fig. 3.1a exhibit *locally* the same mean curvature, whereas the sphere looks *globally* more similar to the center of the ellipsoid.

In Fig. 3.2 however, the local value of mean curvature half-density relates the global appearance of the sphere to the center of the ellipsoid.

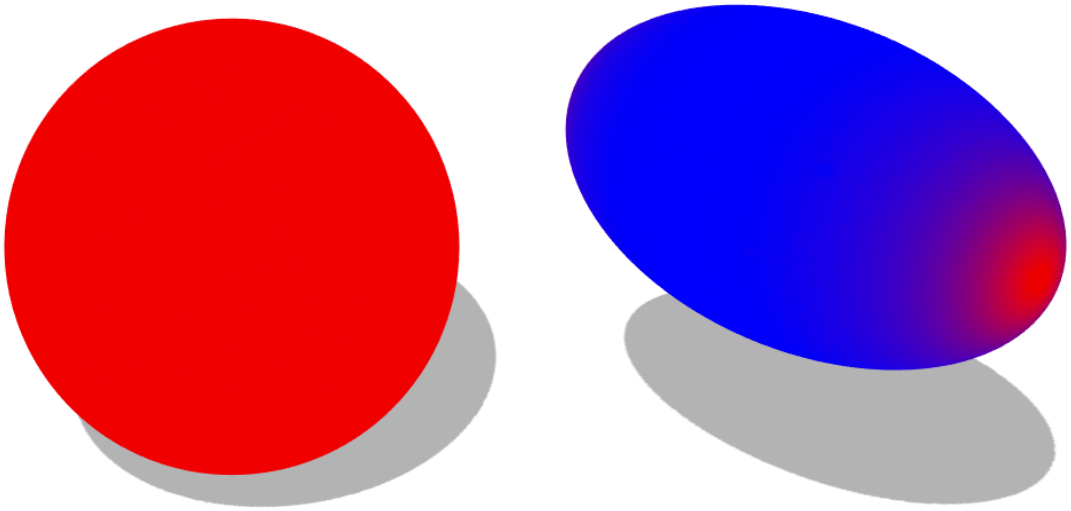

(a) Sphere with radius $R = 0.5$ relative units

(b) Ellipsoid with $(R_x, R_y, R_z) = (2, 1, 1)$ relative units

Figure 3.1: Comparison of mean curvatures as a descriptor of global shape appearance for the sphere and an ellipsoid on a linear scale from 0.6 (blue) to 2.0 (red). The sphere looks globally similar to the center of the ellipsoid, but mean curvature locally coincides with the tip of the ellipsoid.

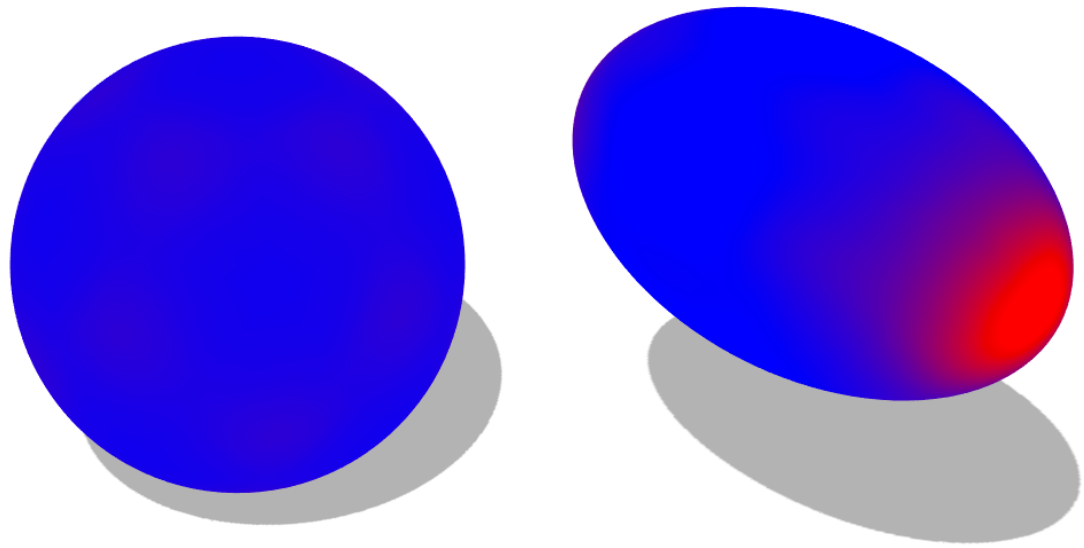

(a) Sphere with radius $R = 0.5$ relative units

(b) Ellipsoid with $(R_x, R_y, R_z) = (2, 1, 1)$ relative units

Figure 3.2: Comparison of mean curvature half-densities as a descriptor of global shape appearance for the sphere and an ellipsoid on a linear scale from 0.05 (blue) to 0.1 (red). Local values in mean curvature half-densities bring the sphere in correspondence with the center of the ellipsoid, which is in accordance with global shape appearance.

3.2 The notion of spin equivalence and integrability

Consider two immersions f and $\tilde{f}$, whose tangent spaces are related by a quaternion similarity transformation, namely that there exists a $\lambda : M \to \mathbb{H} \setminus \{0\}$ such that

$$d\tilde{f} = \overline{\lambda} df \lambda. \tag{3.4}$$

In light of [14], we call this transformation a *spin transformation* and we call immersions f and $\tilde{f}$ *spin equivalent*. Spin equivalence is indeed an equivalence relation. As outlined in Chapter 2, a conformal deformation can be locally expressed as a rotation with scaling in tangent space. Precisely these two operations are encoded in Eq. (3.4): rotation by the unit quaternion $\lambda/|\lambda|$ and scaling by $|\lambda|^2$. In fact, in the case of M being closed and simply connected, *any* two conformal immersions are spin-equivalent.
However, not for every $\lambda : M \to \mathbb{H} \setminus \{0\}$ there is a spin transformation that leads to an *integrable* immersion. In the language of differential forms, $d\tilde{f}$ has to be an exact 1-form. On a simply connected domain every closed form is exact[16] ([14]). To find an *integrability condition*, we therefore have to find conditions under which $d(d\tilde{f}) = 0$.

Theorem 3.1 ([14])**.** *Given a conformal immersion $f : M \to \mathbb{R}^3$ of a closed and simply connected surface M, an immersion $\tilde{f} : M \to \mathbb{R}^3$ can be obtained via spin transformation $d\tilde{f} = \overline{\lambda} df \lambda$ for $\lambda : M \to \mathbb{H} \setminus \{0\}$, if there exists a function $\rho : M \to \mathbb{R}$ such that*

$$-df \wedge d\lambda = \rho \lambda |df|^2 . \tag{3.5}$$

Proof. Using the Leibniz rule Eq. (2.30),

$$d\tilde{f} = d(\overline{\lambda} df \lambda) = d\overline{\lambda} \wedge df\lambda - \overline{\lambda} df \wedge d\lambda = -2\mathrm{Im}(\overline{\lambda} df \wedge d\lambda),$$

which implies that if $\overline{\lambda} df \wedge d\lambda$ is a 2-form that takes values in the purely real quaternions, then $d\tilde{f} = 0$, which means that $d\tilde{f}$ is closed and as M is simply connected, $d\tilde{f}$ is integrable.
As stated in Eq. (2.22), any 2-form is a rescaled version of the volume form by a quaternion-valued function, which in this case has to be purely real, $\overline{\lambda} df \wedge d\lambda = \hat{\rho}|df|^2$. Multiplying by λ and setting $\rho = -\hat{\rho}/|\lambda|^2$, we obtain that there has to exist a function $\rho : M \to \mathbb{R}$ such that

$$-df \wedge d\lambda = \rho \lambda |df|^2 .$$

□

[16] As $d^2 = 0$, the reverse is always true: every exact form is closed.

For a given λ, such a function ρ is *unique*, if it exists ([14]). Note that the theorem is not true for non-simply connected surfaces. A way to successfully apply spin transformations to higher genus surfaces is outlined in [4].

If $f, \tilde{f}$ are related by a spin transformation via λ that fulfills the integrability condition (3.5) for some ρ, we will at times write that f and $\tilde{f}$ are (λ, ρ)-spin equivalent or just λ-spin equivalent.

It is useful to exploit some properties of spin transformation:

Theorem 3.2 ([14])**.** *Let $f, \tilde{f} : M \to \mathbb{R}^3$ be (λ, ρ)-spin equivalent. Then,*

1. *$\tilde{N} = \lambda^{-1} N \lambda$ is the oriented normal to $\tilde{f}$*
2. *$|d\tilde{f}|^2 = |\lambda|^4 |df|^2$*
3. *$\tilde{H} = \frac{H+\rho}{|\lambda|^2}$*

Remark 3.3. The second property (conformal factor) demonstrates that for $|\lambda| \equiv 1$ we obtain an *isometric* spin transformation. Due to the third property, ρ has the interpretation of a *change* in mean curvature half-density, which we will henceforth denote as the *curvature potential*. The mean curvatures of spin equivalent surfaces are related by

$$\tilde{H}|d\tilde{f}| = H|df| + \rho|df|\,. \tag{3.6}$$

Spin transformation is the central tool to navigate in conformal shape space, which is introduced in Chapter 3.4. For our purpose of characterizing isometric deformations, the second property in Theorem 3.2 is the core insight.

3.3 Quaternionic Dirac operator

The integrability condition Eq. (3.5) can be reformulated by introducing the *quaternionic Dirac operator*[17] defined as

$$\mathcal{D}_f := -\frac{df \wedge d\lambda}{|df|^2}. \tag{3.7}$$

Then according to Theorem 3.1, on a simply connected surface M, a spin transformation with $\lambda : M \to \mathbb{H} \setminus \{0\}$ is integrable if and only if there exists some $\rho : M \to \mathbb{R}$ such that

$$(\mathcal{D}_f - \rho)\lambda = 0. \tag{3.8}$$

On a closed surface M, the Dirac operator can be viewed as a self-adjoint, weakly elliptic operator $\mathcal{D}_f : L^2(M, \mathbb{H}) \to L^2(M, \mathbb{H})$ ([4]). This implies that the operator induces an orthonormal eigenbasis of $L^2(M, \mathbb{H})$ and has a discrete spectrum of real eigenvalues.

[17] In the following, we will at times drop the term *quaternionic*.

In [4], emphasis is drawn to the relation of the Dirac operator to classical operators in vector calculus and differential geometry. Consider a quaternion-valued function ψ in the decomposition Eq. (2.10),

$$\psi = a + df(Y) + bN.$$

The action of the Dirac operator can be summarized in the following scheme having matrix-vector multiplication rules in mind:

$$\mathcal{D}_f\psi = \begin{pmatrix} 0 & -\mathrm{curl} & 0 \\ \mathcal{J}\,\mathrm{grad} & -S & \mathrm{grad} \\ 0 & -\mathrm{div} & 2H \end{pmatrix} \begin{pmatrix} a \\ Y \\ b \end{pmatrix} \tag{3.9}$$

Here, S is the shape operator, H is the mean curvature of the immersion f, $\mathcal{J}$ is the complex structure on M (inducing a 90° counterclockwise rotation) and grad, div and curl are the common vector analysis operators.

This equation makes a strong point for the theory of a quaternionic surface description: with an operator that is an endomorphism on the space of quaternion-valued functions, one can express numerous[18] geometrically interesting operators in classical vector calculus. This means that in contrast to the classical theory, the *type* of mathematical object does not change under the action of a differential operator: a quaternionic function is mapped to a quaternionic function.

The name of this operator stems from the fact that in local coordinates, it is equivalent to the spin-Dirac operator from relativistic quantum mechanics ([4]).

3.4 Conformal shape space

In order to gain intuition about the structure of conformal shape space, we closely follow the exposition given in [4]. Let us define the conformal shape space $\mathcal{M}_f$ as the space of all mean curvature half-densities that can be achieved via some spin transformation $\tilde{f}$ of f:

$$\mathcal{M}_f := \left\{ \rho|df| \;\middle|\; \rho|df| = \tilde{H}|d\tilde{f}| - H|df|, \tilde{f} : M \to \mathbb{R}^3 \right\} \subset \mathcal{H}\,. \tag{3.10}$$

For $\rho|df| \in \mathcal{M}_f$, the integrability condition Eq. (3.8) implies that $(\rho + \gamma)|df| \in \mathcal{M}_f$ for all real eigenvalues γ of $\mathcal{D}_f$. As already mentioned in Chapter 3.3, $\mathcal{D}_f$ has a discrete collection of eigenvalues denoted by $\ldots, \gamma_{-1}, \gamma_0, \gamma_1, \ldots$, where the indices emphasize that there are positive as well as negative eigenvalues. We can then find $(\lambda, \rho + \gamma_k)$-spin equivalent surfaces in direction $|df|$. For the case of M being closed and simply connected, M is topologically equivalent to the sphere $\mathbb{S}^2$. Therefore, by transitivity of spin equivalence, $\mathcal{M}_f$ must be connected, as there is a path in $\mathcal{M}_f$ connecting any two spin equivalent surfaces via the sphere. As a consequence, $\mathcal{M}_f$ can be

[18] A comprehensive list including derivations is given in [4].

sketched as a spiral as depicted in Fig. 3.3.

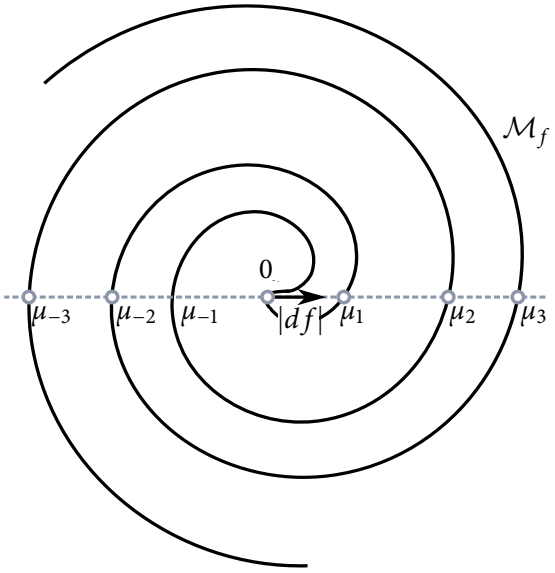

Figure 3.3: Sketch of conformal shape space $\mathcal{M}_f$. One can reach surfaces in direction of $|df|$ via spin transformation represented by mean curvature half-densities μ_i. All surfaces must be globally connected as every closed and simply connected surface is conformally equivalent to the sphere.

Chapter 4

Discretization of Quaternionic Shape Analysis

4.1 Representation of quaternionic calculus in $\mathbb{R}^4$

In order to construct algorithmic applications of quaternionic calculus, a *real* representation is necessary. At the center of this construction is the identification $\mathbb{H} \cong \mathbb{R}^4$, which allows a real representation of the quaternion $q = a + b\mathrm{i} + c\mathrm{j} + d\mathrm{k}$ as a skew-symmetric matrix $\boldsymbol{Q} \in \mathbb{R}^{4\times 4}$ via

$$\boldsymbol{Q} = \begin{pmatrix} a & -b & -c & -d \\ b & a & -d & c \\ c & d & a & -b \\ d & -c & b & a \end{pmatrix}, \tag{4.1}$$

where the basis elements are represented by the Pauli matrices

$$\mathrm{i} = \begin{pmatrix} 0 & -1 & 0 & 0 \\ 1 & 0 & 0 & 0 \\ 0 & 0 & 0 & -1 \\ 0 & 0 & 1 & 0 \end{pmatrix} \quad \mathrm{j} = \begin{pmatrix} 0 & 0 & -1 & 0 \\ 0 & 0 & 0 & 1 \\ 1 & 0 & 0 & 0 \\ 0 & -1 & 0 & 0 \end{pmatrix} \quad \mathrm{k} = \begin{pmatrix} 0 & 0 & 0 & -1 \\ 0 & 0 & -1 & 0 \\ 0 & 1 & 0 & 0 \\ 1 & 0 & 0 & 0 \end{pmatrix}.$$

For the remainder of this section we want to clearly distinguish the levels of continuous operators, quaternionic matrices and their real representation. To this end, we introduce the notational convention of different math fonts. A continuous operator $\mathcal{A} \in L^2(M, \mathbb{H})$, has a quaternionic matrix representation $A \in \mathbb{H}^{m\times n}$, which itself has a real representation $\boldsymbol{A} \in \mathbb{R}^{4m\times 4n}$. Every quaternion in A is represented by a 4×4 block matrix of the form Eq. (4.1) in $\boldsymbol{A}$.
Quaternionic vectors $\xi \in \mathbb{H}^n$ are printed in regular font, whereas their real representations $\boldsymbol{\xi} \in \mathbb{R}^{4n}$ are printed in bold face. With this notational convention it is at all times clear what level of discretization is considered.

As the real representation encodes the algebraic structure of the quaternions, it can be used to express all operations in quaternionic calculus, in particular the Hamilton product is expressed as a matrix vector product

$$qp \triangleq \boldsymbol{Q}\boldsymbol{p}.$$

The transpose of the real skew-symmetric matrix $\boldsymbol{M} \in \mathbb{R}^{4n\times 4n}$ then corresponds to the hermitian adjoint of the quaternionic matrix $M \in \mathbb{H}^{m\times n}$,

$$M^\dagger \triangleq \boldsymbol{M}^T .$$

A quaternionic hermitian matrix $M \in \mathbb{H}^{n\times n}$ has an eigensolution $(\gamma, \xi) \in \mathbb{R} \times \mathbb{H}^n$ if and only if its symmetric real representation $\boldsymbol{M} \in \mathbb{R}^{4n\times 4n}$ has an eigensolution $(\gamma, \boldsymbol{\xi}) \in (\mathbb{R} \times \mathbb{R}^{4n})$.
A real symmetric matrix $\boldsymbol{M} \in \mathbb{R}^{4n\times 4n}$ induces an orthonormal eigenbasis of $\mathbb{R}^{4n}$, a hermitian matrix $M \in \mathbb{H}^n$ however induces an orthonormal eigenbasis of $\mathbb{H}^n$ by Theorem 2.4. Those two concepts are united by Theorem 2.6, which states that for any non-zero $w \in \mathbb{H}^n$, $(\gamma, \xi w)$ is also an eigensolution to the quaternionic matrix M, if (γ, ξ) is one. As a result, every quaternionic eigenvector corresponds to 4-dimensional real eigenspace representation. If we require normalization of the eigenvectors there are still three degrees of freedom left. The interpretation of this mathematical fact in our context is that any solution to a quaternionic eigenvalue problem can only be *unique up to global rotation*.

We represent discrete surfaces by a triangular mesh (V, F), where V is the set of vertex positions with cardinality $|V|$ and F is the face set with cardinality $|F|$ encoding which vertices form a triangle. Discrete quantities in this thesis are either vertex- or face-valued.
An effect to keep in mind when dealing with quaternions on discrete surfaces is the increased memory use. A quaternionic matrix $A \in \mathbb{H}^{|V|\times|V|}$ requires 16 times more memory than a real matrix $\boldsymbol{A} \in \mathbb{R}^{|V|\times|V|}$.

4.2 Discrete Dirac operator

In order to discretize the Dirac operator, we choose a Finite Element approach as in [4].
In general, discretizing an operator $\mathcal{A}$ amounts to weighted integration of its action on piecewise linear functions ϕ over the mesh[19]. We choose uniform integration weights, i.e. integrals are normalized by the total integration area. If A is the matrix representation of the operator $\mathcal{A}$, then applying A to ϕ (considered as a vector) should be equal to the average action of the continuous operator:

$$A\phi = \frac{1}{v(\Omega)} \int_\Omega \mathcal{A}\phi \, dv ,$$

[19] We are considering *linear* Finite Elements. In general, a Finite Element approach can be based on higher order functions.

where Ω is the integration domain and ν the surface measure.

As a starting point for discretizing the Dirac operator we choose the rewritten continuous expression

$$\mathcal{D}_f \lambda = \frac{d(df\lambda)}{|df|^2}.$$

Let f and λ be piecewise linear functions that are interpolated between the mesh vertices. Face-wise integration of $\mathcal{D}_f\lambda$ over a triangle t_l with vertices (i, j, k) and edges $e_k := e_{ij} = f_j - f_i$ (cf. Fig. 4.1) yields by Stokes' theorem Eq. (2.25)

$$\begin{aligned}\frac{1}{A_l}\int_{t_l} \mathcal{D}_f\lambda |df|^2 &= \frac{1}{A_l}\int_{\partial t_l} df\lambda = \frac{1}{A_l}\sum_{e_{ij}\in\partial t_l}(f_j - f_i)\frac{\lambda_i+\lambda_j}{2} \\ &= \frac{1}{A_l}\left[(e_{ij}+e_{ki})\frac{\lambda_i}{2} + (e_{jk}+e_{ij})\frac{\lambda_j}{2} + (e_{jk}+e_{ki})\frac{\lambda_k}{2}\right] \\ &= -\frac{1}{2A_l}(e_i\lambda_i + e_j\lambda_j + e_k\lambda_k),\end{aligned}$$

which gives the discretized matrix representation $D \in \mathbb{H}^{|F|\times|V|}$ of the Dirac operator as

$$D_{ij} = -\frac{1}{2A_i}e_j. \tag{4.2}$$

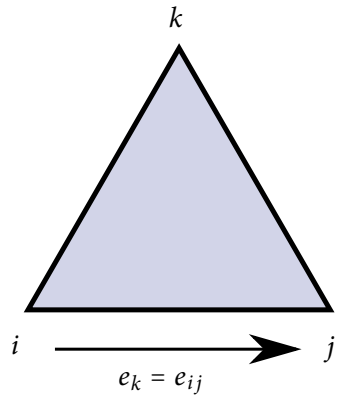

Figure 4.1: Sketch for the notation of a triangle of the discretized surface. The edge e_{ij} can be described as connecting vertices i and j or as being across of vertex k, when it is denoted as e_k.

4.3 Discrete curvature potential

Throughout this thesis, we will represent the discrete version of the curvature potential ρ by a vertex-valued function[20]. For the Finite Element discretization, let ρ and λ be piecewise linear

[20] In contrast, in parts of [4], a face-wise representation is used.

functions interpolated between the vertices. Then,

$$\frac{1}{A_l}\int_{t_l}\rho\lambda|df|^2 = \frac{1}{3}\sum_{v_i\in t_l}\lambda_i\rho_i\,.$$

Consequently, the matrix representation $R\in\mathbb{H}^{|F|\times|V|}$ is

$$R_{ij} = \frac{1}{3}\rho_j\mathbf{1}_{\{v_j\in t_i\}}\,. \tag{4.3}$$

4.4 Adjoint matrices

The hermitian adjoint of a continuous linear operator $\mathcal{A}:\mathfrak{H}\to\mathfrak{H}$ on a Hilbert space $\mathfrak{H}$ is the continuous, linear operator $\mathcal{A}^*:\mathfrak{H}\to\mathfrak{H}$, which is uniquely defined by the expression

$$\langle\mathcal{A}x,y\rangle = \langle x,\mathcal{A}^*y\rangle \qquad \forall x,y\in\mathfrak{H}.$$

In our setting, the Hilbert space is $L^2(M,\mathbb{H})$ with the corresponding *surface measure*. In the discrete case, this Hilbert space is $\mathbb{H}^{|V|}$ or $\mathbb{H}^{|F|}$. When choosing the inner product on theses spaces, we have to make sure that the surface area is accounted for, even though the appearing functions are vertex-valued only. Therefore, the inner product between two vertex-valued vectors $a,b\in\mathbb{R}^{|V|}$ *cannot* be the standard inner product[21], but has to be *reweighted* by suitable surface areas.
In general, on $\mathbb{R}^n$, any positive definite symmetric matrix $\boldsymbol{M}$ defines an inner product

$$\langle\cdot,\cdot\rangle:\mathbb{R}^n\times\mathbb{R}^n\to\mathbb{R},(\boldsymbol{x},\boldsymbol{y})\mapsto\boldsymbol{x}^T\boldsymbol{M}\boldsymbol{y}\,.$$

In our context, we would like that $\boldsymbol{M}$ represents the surface weight, meaning that $\mathbf{1}^T\boldsymbol{M}\mathbf{1}$ equals the total surface area.

On $\mathbb{H}^{|V|}$, this can be realized by choosing the real diagonal matrix

$$(M_V)_{ii} = \frac{1}{3}\sum_{k\in\mathcal{F}_i}A_k,$$

where A_k is the area of face $k\in F$. This corresponds to the Voronoi areas on the diagonal.
For an inner product on $\mathbb{H}^{|F|}$, we define the real diagonal matrix

$$(M_F)_{kk} = A_k,$$

the matrix with face areas on the diagonal.

[21] This would correspond to the Dirac measure on the surface with atoms at the vertices.

Equipped with this inner product, the hermitian mesh adjoint of an operator $E \in \mathbb{H}^{|F|\times|V|}$ is given by

$$E^* = M_V^{-1} E^\dagger M_F,$$

where $E^\dagger$ is the hermitian matrix adjoint, namely transposed and quaternion conjugated.
In this thesis we adopt this as a *notational convention*: mesh adjoints of a quaternionic hermitian matrix A are specified by a A^*, matrix adjoints are denoted by $A^\dagger$.

4.5 Discrete Dirac equation

With the quantities derived in the previous sections, we are now able to discretize the time-independent Dirac equation

$$(\mathcal{D}_f - \rho)\lambda = \gamma\lambda.$$

With $A := (D - R) \in \mathbb{H}^{|F|\times|V|}$, the most straightforward idea would be to formulate the discretized *rectangular* eigenvalue problem $A\lambda = \gamma B\lambda$, where $B \in \mathbb{H}^{|F|\times|V|}$ with $B_{ij} = \frac{1}{3}\,\mathbf{1}_{\{v_j \in t_i\}}$ as an averaging operator. As *square* eigenvalue problems are easier to deal with it would be possible to average faces back to vertices. In [4] it is noted though that this approach heavily modifies solutions. We will outline the author's proposed solution to this issue in the following.

In the continuous case, any eigensolution (γ, λ) to the equation $\mathcal{A}\lambda = \gamma\lambda$ is also a solution to the equation $\mathcal{A}^2\lambda = \gamma^2\lambda$, though the reverse is not true, as we lose the *sign* of γ. Introducing the operator $\mathcal{A}$ in addition on the right-hand side discriminates between the sign of the eigenvalues. This leads to the discrete *square* eigenvalue problem

$$A^* A\lambda = \gamma B^* A\lambda\,.$$

We have now traded a *rectangular* eigenvalue problem with a *generalized*, but *square* eigenvalue problem. In practice, this can be reduced to a standard eigenvalue problem since we are looking for the smallest eigenvalue and can neglect mixing eigenspaces due to the sign ambiguity. We therefore seek to solve the standard eigenvalue problem

$$A^* A\lambda = \gamma\lambda\,. \tag{4.4}$$

It is convenient to build the matrix $E := A^* A$ by directly looping over the faces. In particular, for each pair of vertices (i, j) there are two faces k_1, k_2 that include *both* vertices (cf. Fig. 4.2), i.e.

$$E_{ij} = \sum_{k\in\{k_1,k_2\}} -\frac{e_i^{(k)} e_j^{(k)}}{4A_k} + \frac{1}{6}(\rho_i e_j^{(k)} - \rho_j e_i^{(k)}) + \frac{A_k}{9}\rho_i\rho_j\,. \tag{4.5}$$

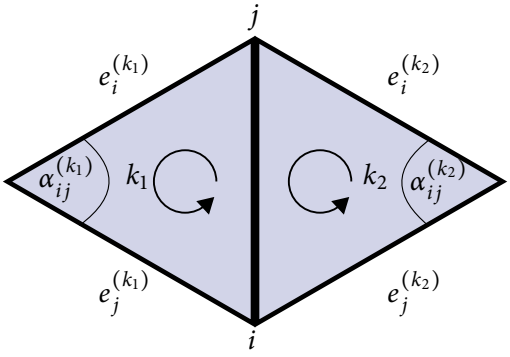

Figure 4.2: Sketch of two triangles to an edge connecting vertices i and j.

4.6 Discrete spin transformation: recovering vertex coordinates

To recover the vertex positions, the spin transformation equation $d\tilde{f} = \overline{\lambda} df \lambda$ has to be solved for new coordinates $\tilde{f}$. We follow the approach outlined in [4].
According to the quaternion similarity transformation, the new edges $\tilde{e}_{ij} := \tilde{f}_j - \tilde{f}_i$ should be obtained by scaling and rotating the original edges $e_{ij} := f_j - f_i$ according to λ. The similarity transformation is discretized by integrating $\overline{\lambda} df \lambda$ over each edge in the original mesh under the assumption that λ is a piecewise linear function interpolated between the vertices:

$$\tilde{e}_{ij} = \frac{1}{3}\overline{\lambda}_i e_{ij} \lambda_i + \frac{1}{6}\overline{\lambda}_i e_{ij} \lambda_j + \frac{1}{6}\overline{\lambda}_j e_{ij} \lambda_i + \frac{1}{3}\overline{\lambda}_j e_{ij} \lambda_j \,. \tag{4.6}$$

Subsequently, we solve the linear system $d\tilde{f} = \tilde{e}$ for the vertex coordinates $\tilde{f}$ in a least-squares approach,

$$\tilde{f} = \underset{\tilde{f} \in \mathbb{R}^3}{\arg\min} \int_M |\nabla \tilde{f} - \tilde{e}|^2 |d\tilde{f}|^2 \,. \tag{4.7}$$

To this end, we solve the associated Euler-Lagrange equation, which is the Poisson problem

$$\Delta \tilde{f} = \nabla \tilde{e} \,. \tag{4.8}$$

For the discretization of the Laplace-Beltrami operator Δ and the derivative operator ∇, we use the cotangent weight scheme obtained with a Finite Element approach.
Note that even though in continuous theory $d\tilde{f}$ is an exact 1-form, we still have to solve a least-squares problem in this step, as the exact integrability is lost due to the discretization in Eq. (4.6). However, as mentioned in [4], the residual $r := |d\tilde{f} - \tilde{e}|^2$ vanishes under mesh refinement and even on a coarse level this method yields good results.

4.7 Mean curvature and mean curvature half-density

We calculate the mean curvature normal at a vertex with coordinates f_i as introduced in [7]:

$$H_i N_i = -\frac{1}{4A_i} \sum_{j \in \mathcal{N}_i} (\cot(\alpha_{ij}^{(k_1)}) + \cot(\alpha_{ij}^{(k_2)}))(f_j - f_i), \tag{4.9}$$

where H_i is the mean curvature, N_i is the outer unit normal, A_i is the Voronoi area and the angles $\alpha_{ij}^{(k)}$ are as depicted in Fig. 4.3. The summation is taken over the one-ring neighborhood $\mathcal{N}_i$. It follows that the mean curvature at a vertex i is calculated as the projection onto the outer unit normal

$$H_i = \left\langle N_i, -\frac{1}{4A_i} \sum_{j \in \mathcal{N}_i} (\cot(\alpha_{ij}^{(k_1)}) + \cot(\alpha_{ij}^{(k_2)}))(f_j - f_i) \right\rangle . \tag{4.10}$$

If the Laplace-Beltrami operator Δ is discretized via the cotangent scheme, this relation may be formulated as

$$H_i = \langle N_i, (\Delta f)_i \rangle . \tag{4.11}$$

Mean curvature half-density is equivalent to mean curvature rescaled by a length scale on the surface, as discussed in Chapter 3.1. For a discrete mesh, the common length scale on a triangle with area A is $\sqrt{A}$. As a consequence, we calculate mean curvature half-density by

$$(H|df|)_i = \left\langle N_i, -\frac{1}{4\sqrt{A_i}} \sum_{j \in \mathcal{N}_i} (\cot(\alpha_{ij}^{(k_1)}) + \cot(\alpha_{ij}^{(k_2)}))(f_j - f_i) \right\rangle . \tag{4.12}$$

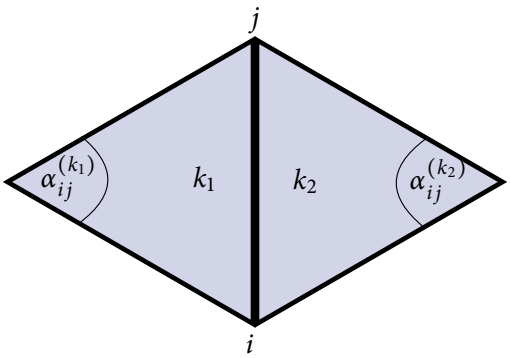

Figure 4.3: Illustration of the quantities involved in the computation of the mean curvature normal.

Chapter 5

The Dirac operator eigenvalue problem under spin transformation

5.1 Motivation: Laplace-Beltrami operator as an isometry-invariant

In Chapter 1.2, we argued that the most suitable class for physical deformations is that of *isometries*. A general approach for establishing a correspondence between two isometric surfaces is to find a suitable *invariant under isometric deformation* and to relate points that have the same properties with respect to this invariant. This *shape matching* problem is one of the classical problems in Shape Analysis.
More precisely, consider two isometric surfaces M_1 and M_2 with a bijective map $T : M_1 \to M_2$. The simplest invariants are functions $\psi_i : M_i \to \mathbb{R}$ that satisfy $\psi_1(p_1) = \psi_2(T(p_1)) \quad \forall p_1 \in M_1$. A concrete example is the Gaussian curvature function $\kappa_i : M_i \to \mathbb{R}$. Note however that Gaussian curvature is not discriminative enough to relate points between the two surfaces, as there could easily be several points on both surfaces with equal Gaussian curvature.

More complex invariants are based on operators $\mathcal{O}_i \in L^2(M_i, \mathbb{R})$ and a *functional transformation* $\mathcal{T} : L^2(M_1, \mathbb{R}) \to L^2(M_2, \mathbb{R}), \varphi \mapsto \varphi \circ T^{-1}$, where $T : M_1 \to M_2$ is the bijective map in the above sense, such that

$$\mathcal{O}_1(\varphi_1) = \mathcal{O}_2(\mathcal{T}(\varphi_1)) \,. \tag{5.1}$$

The most successful isometry-invariant operator has been the Laplace-Beltrami operator $\mathcal{O}_i = \Delta_g^{(i)}$, which depends only on the *metric* g ([22]). The equality

$$\Delta_g^{(1)} \varphi_1 = \Delta_g^{(2)}(\mathcal{T}(\varphi_1)) \tag{5.2}$$

holds for all scalar functions $\varphi_1 \in L^2(M_1, \mathbb{R})$ if and only if $\mathcal{T}$ is the functional representation of an isometry, that is, the associated mapping T induces an isometric deformation. Build on top of this idea is the concept of *functional maps*, which was first introduced in [18], and has led to fruitful

research in the field of Shape Analysis.

5.2 Spin transformation of the Dirac operator eigenvalue problem

Motivated by the success story of the Laplace-Beltrami operator as an isometry-invariant, we want to analyze how the eigenvalue system of the Dirac operator changes under spin transformation. The goal is then to infer properties of the spin transformation from the Dirac operators based on two spin equivalent shapes.

For a given conformal immersion $f : M \to \mathbb{R}^3$ with λ-spin equivalent immersion $\tilde{f}$ we will see how the Dirac operator $\mathcal{D}_{\tilde{f}}$ derived from $\tilde{f}$ acts on eigenfunctions of the Dirac operator $\mathcal{D}_f$, which is derived from the original immersion f. To this end, we apply the computation methods for quaternionic differential forms, which are introduced in Chapter 2.2.3. For eigenfunctions ϕ of $\mathcal{D}_f$, the operator $\mathcal{D}_{\tilde{f}}$ is applied to the function $\overline{\lambda}\phi$ instead of solely ϕ, as this leads to a result, which has natural mathematical interpretation. This result is summarized in the following theorem.

Theorem 5.1. *Let $f : M \to \mathrm{Im}(\mathbb{H})$ be a conformal immersion and let $\tilde{f} : M \to \mathrm{Im}(\mathbb{H})$ be an immersion obtained via the spin transformation $d\tilde{f} = \overline{\lambda} df \lambda$ for $\lambda : M \to \mathbb{H} \setminus \{0\}$, which solves $(\mathcal{D}_f - \rho)\lambda = 0$ for some $\rho : M \to \mathrm{Re}(\mathbb{H})$. Let $\phi : M \to \mathbb{H}$ be an eigenvector of $\mathcal{D}_f$ to the eigenvalue $\gamma \in \mathrm{Re}(\mathbb{H})$.*
Then,

$$\mathcal{D}_{\tilde{f}}(\overline{\lambda}\phi) = \frac{\overline{\lambda}\mathcal{D}_f(|\lambda|^2)\phi}{|\lambda|^4} + \frac{(\gamma - \rho)}{|\lambda|^2}\overline{\lambda}\phi. \tag{5.3}$$

Proof. We use the wedge product rules for quaternionic differential forms, Eqs. (2.28), the properties of spin transformations listed in Theorem 3.2, as well as the Leibniz rule for quaternionic differential forms, Eq. (2.30), in the form

$$d(|\lambda|^2) = d(\lambda\overline{\lambda}) = (d\lambda)\overline{\lambda} + \lambda d\overline{\lambda}. \tag{5.4}$$

The integrability condition yields a substitution of the action of $\mathcal{D}_f$ on λ as $\mathcal{D}_f(\lambda) = \lambda\rho$. Furthermore, we use that every 0-form commutes with the Hodge star operator.
Altogether this leads to the following derivation:

$$
\begin{aligned}
\mathcal{D}_{\tilde{f}}(\overline{\lambda}\phi) &= \frac{-\overline{\lambda}df\lambda \wedge d(\overline{\lambda}\phi)}{|d\tilde{f}|^2} \\
&= -\overline{\lambda}\frac{df \wedge \lambda d(\overline{\lambda}\phi)}{|d\tilde{f}|^2} \\
&= -\overline{\lambda}\frac{df \wedge \lambda(d(\overline{\lambda})\phi + \overline{\lambda}d\phi)}{|d\tilde{f}|^2} \\
&= -\overline{\lambda}\left[\frac{df \wedge \lambda d\overline{\lambda}}{|d\tilde{f}|^2}\phi + \frac{df \wedge |\lambda|^2 d\phi}{|d\tilde{f}|^2}\right] \\
&= -\frac{\overline{\lambda}}{|\lambda|^4}\left[\frac{(df \wedge d\lambda)}{|df|^2}(-\overline{\lambda}\phi) + \frac{df \wedge d(|\lambda|^2)}{|df|^2}\phi + \frac{df \wedge d\phi}{|df|^2}|\lambda|^2\right] \\
&= \frac{\overline{\lambda}}{|\lambda|^4}[-\mathcal{D}_f(\lambda)\overline{\lambda}\phi + \mathcal{D}_f(|\lambda|^2)\phi + \mathcal{D}_f(\phi)|\lambda|^2] \\
&= \frac{\overline{\lambda}}{|\lambda|^4}(-\rho\lambda\overline{\lambda}\phi + \mathcal{D}_f(|\lambda|^2)\phi + \gamma\phi|\lambda|^2) \\
&= \frac{\overline{\lambda}\mathcal{D}_f(|\lambda|^2)\phi}{|\lambda|^4} + \frac{(\gamma-\rho)}{|\lambda|^2}\overline{\lambda}\phi\,.
\end{aligned}
$$

□

It is worth drawing attention to special cases of Theorem 5.1 that carry geometric meaning. If λ is a norm-constant quaternion-valued function, $|\lambda(p)| = c \in \mathbb{R}\ \forall p \in M$, then $\mathcal{D}_f(|\lambda|^2) = 0$, which implies that $\overline{\lambda}\phi$ is a generalized eigenvector of $\mathcal{D}_{\tilde{f}}$. In particular, this is the case for isometric deformations with $c = 1$. If λ is a constant quaternion, then $\rho = 0$ and one obtains the case of rigid scaling, implying that $\overline{\lambda}\phi$ is an eigenvector of $\mathcal{D}_{\tilde{f}}$ to the eigenvalue $\gamma \in \mathbb{R}$. This case corresponds to a global rotation and scaling.

Consider the result derived for an isometric deformation,

$$
\mathcal{D}_{\tilde{f}}(\overline{\lambda}\phi_k) = (\gamma_k - \rho)\overline{\lambda}\phi_k \qquad \forall k \in \mathbb{N}\,, \tag{5.5}
$$

which gives us infinitely many equations, as $\{\phi_k\}_{k\in\mathbb{N}}$ forms a basis of $L^2(M, \mathbb{H})$.
Whereas this result can in theory be used to establish a correspondence between a shape and an isometric deformation thereof by solving for the spin transformation λ, in practice this leads to a chicken-and-egg-problem, as one has to know a correspondence between the two shapes to align the matrices derived from the operator $(\mathcal{D}_{\tilde{f}} - \rho)$ with the vectors ϕ derived from the original immersion f. Furthermore, already to establish the curvature potential ρ, the correspondence between the two shapes has to be known.
Even under the assumption that a correspondence is given, which implies that the curvature potential ρ is known, Eq. (5.5) does not offer new information. The corresponding λ can be found

by directly considering the spin transformation Eq. (3.4) together with the integrability condition Eq. (3.8), since a spin transformation pairing (λ, ρ) is *unique*, if it exists ([14]).
As a consequence, Theorem 5.1 does not imply a new method for inferring a transformation in the isometric case.
However, it remains an open problem whether the first term in Eq. (5.3) can be used to quantify the deviation from isometry.

Chapter 6

Spectral geometry of the squared Dirac operator

As outlined in Chapter 5.1, the Laplace-Beltrami operator is invariant under isometric deformation. Furthermore, as an essentially self-adjoint operator on $L^2(M, \mathbb{R})$ of a surface M, it induces an eigenbasis of $L^2(M, \mathbb{R})$ ([22]). As a consequence, two isometric surfaces can be put in correspondence via *spectral* properties of their Laplace-Beltrami operators, most notably the heat kernel ([23],[24],[1]). In fact, the Laplace-Beltrami eigenbasis carries the complete *intrinsic geometric* information ([22]). This informative property carries over to the discrete case ([28]).
As the Laplace-Beltrami operator is central to the diffusion equation, methods of recovering geometric information from its eigenbasis are commonly summarized under the term *diffusion geometry*. For the Dirac operator, we use the more general term *spectral geometry*.

Dirac operators generally have the property that their square can be related to the Laplace-Beltrami operator and it is therefore appealing for our purposes to analyze this relation in detail.
It turns out that the Laplace-Beltrami operator can be recovered in the quaternionic framework, a result which is outlined in [4] and stated for the general case in Theorem 6.1 and for an interesting special case in Corollary 6.3.
Consequently, the Quaternionic Shape Analysis framework can provide a *superset* of methods beyond Laplace-Beltrami diffusion geometry.
In particular, Laplace-Beltrami diffusion geometry can potentially be complemented by quantities related to the *extrinsic geometry*.

Theorem 6.1 ([4]). *Let $f : M \to \mathbb{R}^3$ be a conformal immersion that induces a Riemannian metric g_f and let $\psi : M \to \mathbb{H}$ be a smooth quaternionic function. Then*

$$\mathcal{D}_f^2 \psi = \Delta_{g_f} \psi + \frac{dN \wedge d\psi}{|df|^2}. \tag{6.1}$$

Proof. By definition of the Dirac operator,

$$|df|^2 \mathcal{D}_f \psi = -df \wedge d\psi. \tag{6.2}$$

Using Eq. (2.36) together with identity (2.33) for the wedge product, we arrive at

$$-df df \mathcal{D}_f \psi = -df \star d\psi + (\star df) d\psi.$$

As the immersion f is conformal, we have $\star df = N df = -df N$ and dividing by $-df$ then yields

$$df \mathcal{D}_f \psi = \star d\psi + N d\psi.$$

Applying the exterior derivative on both sides and using the Leibniz rule, we obtain

$$-df \wedge d(\mathcal{D}_f \psi) = d \star d\psi + dN \wedge d\psi. \tag{6.3}$$

The left-hand side of Eq. (6.3) now resembles the right-hand side of Eq. (6.2) and we can re-substitute to obtain

$$|df|^2 \mathcal{D}_f^2 \psi = d \star d\psi + dN \wedge d\psi\,.$$

As $1/|df|^2$ is the Hodge star operator on 2-forms, finally

$$\mathcal{D}_f^2 \psi = \star d \star d\psi + \frac{dN \wedge d\psi}{|df|^2}$$

and the Laplace-Beltrami operator appears in its exterior calculus disguise, $\Delta_{g_f} = \star d \star d$. □

In particular, for a real valued function $\psi : M \to \mathbb{R}$, we recover the Laplace-Beltrami operator acting on $L^2(M, \mathbb{R})$.
For this insight, we have to show that the second term in Eq. (6.1) has no scalar contribution, when the squared Dirac operator is applied to real valued functions.

Lemma 6.2. *For $\psi : M \to \mathbb{R}$, $\frac{dN \wedge d\psi}{|df|^2}$ is tangent-valued.*

Proof. Let $X \in TM$ be a unit vector field. Then

$$dN \wedge d\psi(X, \mathcal{J}X) = dN(X) d\psi(\mathcal{J}X) - dN(\mathcal{J}X) d\psi(X).$$

Since for the Gauss map, we have $|N(p)| = 1$, $\forall\, p \in M$, it follows that $\langle dN(X), N \rangle = 0$ $\forall X \in TM$, i.e. dN is tangent-valued. As ψ is real valued, the differential $d\psi$ is real valued, and it follows that $dN \wedge d\psi(X, \mathcal{J}X)$ is tangent-valued. □

We obtain the following corollary from Theorem 6.1 and Lemma 6.2.

Corollary 6.3. *Let $f : M \to \mathbb{R}^3$ be a conformal immersion that induces a Riemannian metric g_f and let $\psi : M \to \mathbb{R}$ be a smooth real valued function, then*

$$\mathrm{Re}(\mathcal{D}_f^2 \psi) = \Delta_{g_f} \psi \,. \tag{6.4}$$

6.1 Recovering Laplace-Beltrami diffusion geometry for discrete surfaces

Given the discretization of the Dirac operator as introduced in Chapter 4.2, Corollary 6.3 induces a discretization of the Laplace-Beltrami operator. It is natural to inquire *which* particular discretization this is. This question is non-trivial as can be seen for example in [27], which offers a comparison of several discretizations of the Laplace-Beltrami operator.

We prove that the discretization we obtain through Eq. (6.4) is the commonly used cotangent Laplacian (cf. [20]). A modern overview of the cotangent formula is given in [26]. Note that the cotangent discretization of the Laplace-Beltrami operator is within the Finite Element paradigm, which is also used for the discretization of the Dirac operator as introduced in Chapter 4.2.

Our result, as summarized in Theorem 6.4, can therefore be interpreted as a consistency result for the Finite Element method, which allows us to *compute* methods based on Laplace-Beltrami diffusion geometry *directly* from within the quaternionic framework.

Theorem 6.4. *Define $D \in \mathbb{H}^{|F|\times|V|}$ by $D_{ij} = -\frac{1}{2A_i} e_j^{(i)}$, where A_i is the area of face i and $e_j^{(i)}$ is the oriented edge quaternion across vertex j in face i (cf. Fig. 6.1). Further denote its adjoint $D^* \in \mathbb{H}^{|V|\times|F|}$ by $D^* = M_V^{-1} D^\dagger M_F$, where $M_V \in \mathbb{H}^{|V|\times|V|}$ is defined by $(M_V)_{ij} = \sum_{m\in\mathcal{F}_i} \frac{1}{3} A_m \delta_{ij}$ and $M_F \in \mathbb{H}^{|F|\times|F|}$ by $(M_F)_{ij} = A_i \delta_{ij}$. Then for any $\varphi \in \mathrm{Re}(\mathbb{H}^{|V|})$,*

$$\mathrm{Re}\big((D^* D)\varphi\big)_i = \sum_{j=1}^{|V|} \frac{1}{A_i^{\mathrm{Voronoi}}} w_{ij} \varphi_j \tag{6.5}$$

with weights

$$w_{ij} = \begin{cases} \frac{1}{2}\big(\cot(\alpha_{ij}^{(k_1)}) + \big(\cot(\alpha_{ij}^{(k_2)})\big) & \text{if } i \neq j, j \in \mathcal{N}_i \\ -\sum_{l\neq i} w_{il} & \text{if } i = j \\ 0 & \text{otherwise} \end{cases}$$

Here, k_1, k_2 are the two faces adjacent to the oriented edge connecting vertices i and j with angles $\alpha_{ij}^{(k_1)}, \alpha_{ij}^{(k_2)}$ and $A_i^{\mathrm{Voronoi}} = \sum_{m\in\mathcal{F}_i} \frac{1}{3} A_m$ is the Voronoi area around vertex i.

Proof. For quaternionic calculations, we make use of the relation Eq. (2.4), which relates the quaternionic Hamilton product to vector calculus operations. We readily calculate the adjoint

matrix elements as

$$D^*_{ij} = \sum_{k=1}^{|V|} (M_V^{-1})_{ik} (D^\dagger M_F)_{kj} = \sum_{k=1}^{|V|} \frac{3}{A_i^{\text{ring}}} \delta_{ik} \left(\frac{1}{2A_j} e_k^{(j)} A_j \right) = \frac{3}{2A_i^{\text{ring}}} e_i^{(j)}, \tag{6.6}$$

where $A_i^{\text{ring}} := \sum_{m \in F_i} \frac{1}{3} A_m$. In consequence, the squared Dirac operator matrix elements become

$$(D^* D)_{ij} = \sum_{k=1}^{|F|} D^*_{ik} D_{kj} = -\sum_{k=1}^{|F|} \frac{3}{4A_i^{\text{ring}}} \frac{1}{A_k} e_i^{(k)} e_j^{(k)}. \tag{6.7}$$

We begin by specifying the off-diagonal elements. For every pair of vertices (i, j) with $i \neq j$ there are exactly two faces adjacent to the edge connecting i and j. We call these faces k_1, k_2. Then,

$$(D^* D)_{ij} = -\frac{3}{4A_i^{\text{ring}}} \left(\frac{1}{A_{k_1}} e_i^{(k_1)} e_j^{(k_1)} + \frac{1}{A_{k_2}} e_i^{(k_2)} e_j^{(k_2)} \right). \tag{6.8}$$

Note that in this context the edge vectors $e_j^{(k)}$ are interpreted as (imaginary) quaternions. For purely imaginary quaternions, we read off Eq. (2.5) that

$$e_i^{(k)} e_j^{(k)} = \begin{cases} 2A_k N_k^{(f)} - 2A_k \cot(\alpha_{ij}^{(k)}) & \text{if } k = k_1 \\ -2A_k N_k^{(f)} - 2A_k \cot(\alpha_{ij}^{(k)}) & \text{if } k = k_2\,, \end{cases} \tag{6.9}$$

where $N_k^{(f)}$ is the face normal of triangle k. The sign change in the imaginary part is due to the orientation of the edge vectors, as depicted in Fig. 6.1.

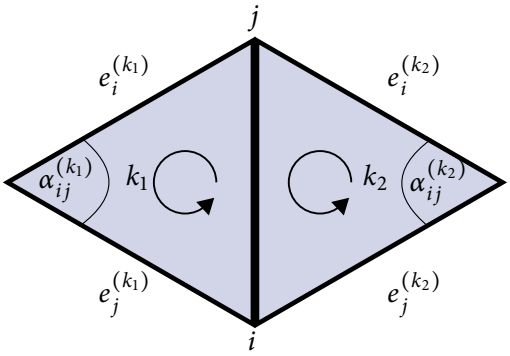

Figure 6.1: Sketch of two triangles to an edge connecting vertices i and j.

Then we obtain

$$\text{Re}\big((D^* D)_{ij}\big) = \frac{3}{2A_i^{\text{ring}}} \big(\cot(\alpha_{ij}^{(k_1)}) + \cot(\alpha_{ji}^{(k_2)})\big). \tag{6.10}$$

As $A_i^{\text{Voronoi}} = \frac{1}{3} A_i^{\text{ring}}$, we arrive at the claimed result for the off-diagonal elements.

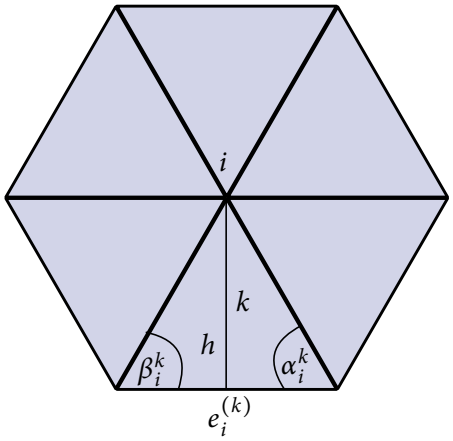

Figure 6.2: 1-ring neighborhood of vertex i with face k, associated angles α_i^k and β_i^k and triangle height h.

For the diagonal elements we use an elementary geometric argument on the 1-ring neighborhood as depicted in Fig. 6.2. We start by rewriting the sum over neighboring vertices to obtain a sum over adjacent faces, as every angle around the 1-ring appears exactly once in the sum:

$$\sum_{j\in\mathcal{N}_i} \frac{1}{2}(\cot(\alpha_{ij}^{(k_1)}) + \cot(\alpha_{ji}^{(k_2)})) = \sum_{k\in\mathcal{F}_i} \frac{1}{2}(\cot(\alpha_i^k) + \cot(\beta_i^k))\,.$$

Suppose the ratio of the edge length of $e_i^{(k)}$ on the side of α_i^k is $x \in (0,1)$. Then with $e := |e_i^{(k)}|$,

$$\frac{1}{2}(\cot(\alpha_i^k) + \cot(\beta_i^k)) = \frac{1}{2}\left(\frac{e(1-x)+ex}{h}\right) = \frac{e}{2h}.$$

As the triangle height h is related to its area A by $h = 2A/e$, it follows that

$$\frac{1}{2}(\cot(\alpha_i^k) + \cot(\beta_i^k)) = \frac{e^2}{4A_k}\,. \tag{6.11}$$

From Eq. (6.7) together with Eq. (6.11) we deduce that

$$\begin{aligned}(D^*D)_{ii} &= -\sum_{k\in\mathcal{F}_i} \frac{1}{A_i^{\text{Voronoi}}} \frac{|e_i^{(k)}|^2}{4A_k} \\ &= -\sum_{k\in\mathcal{F}_i} \frac{1}{2A_i^{\text{Voronoi}}}(\cot(\alpha_i^k) + \cot(\beta_i^k)) \\ &= -\frac{1}{2A_i^{\text{Voronoi}}} \sum_{j\in\mathcal{N}_i} (\cot(\alpha_{ij}^{(k_1)}) + \cot(\alpha_{ji}^{(k_2)})),\end{aligned}$$

and we arrive at the claimed statement for the diagonal elements. □

6.2 Imaginary contribution for real valued functions

In the previous section, we discussed the discrete analog to Eq. (6.4), which corresponds to the real part of Eq. (6.1), when the Dirac operator is applied to real valued functions. We want to complement this discussion by analyzing the imaginary contribution to Eq. (6.1) for real valued functions. Whereas the Laplace-Beltrami operator is an isometric invariant, the imaginary part could potentially provide information about the *extrinsic* geometry of the shape.

Consequently, spectral properties of the Laplace-Beltrami operator and additional extrinsic features can be calculated within the *same* framework.

As an example, along the idea of Quaternionic Shape Analysis as a unified tool for Shape Analysis, the imaginary contribution could be used to distinguish the *intrinsic symmetry* of shapes, a problem that appears in characterizing the intrinsic geometry locally via descriptors derived from the Laplace-Beltrami operator ([24],[1]). Signatures corresponding to intrinsically symmetric points could be complement by *different* extrinsic quantities.

On the contrary, a method to compute global intrinsic symmetries only based on the Laplace-Beltrami eigensystem is devised in [19].

In this section, we give a structural result showing how the imaginary contribution behaves under spin transformation. Exploiting this relation for Shape Analysis purposes remains an open problem for a future research effort.

Let us investigate how this imaginary contribution behaves under spin transformation. To this end, let $a : M \to \mathbb{R}$ be a real valued function on the surface M. Recall from Lemma 6.2 that the imaginary contribution is purely tangent-valued.

According to Theorem 3.2 the Gauss map transforms as $\tilde{N} = \lambda^{-1} N \lambda$, which, using the Leibniz rule Eq. (2.30), yields

$$\begin{aligned}\frac{d\tilde{N} \wedge da}{|d\tilde{f}|^2} &= \frac{d(\lambda^{-1} N \lambda) \wedge da}{|\lambda|^4 |df|^2} \\ &= \frac{d(\lambda^{-1}) N \lambda \wedge da}{|\lambda|^4 |df|^2} + \frac{\lambda^{-1}(dN)\lambda \wedge da}{|\lambda|^4 |df|^2} + \frac{\lambda^{-1} N d\lambda \wedge da}{|\lambda|^4 |df|^2}.\end{aligned}$$

For the special case of an isometric deformation, we have $\lambda^{-1} = \overline{\lambda}$. Furthermore, as exterior differentiation and quaternionic conjugation are linear operations, $d\overline{\lambda} = \overline{d\lambda}$. Using Lemma 6.2

and that for a purely imaginary quaternion $q \in \mathrm{Im}(\mathbb{H})$, $\overline{q} = -q$, it follows that

$$\begin{aligned}\frac{d\tilde{N} \wedge da}{|d\tilde{f}|^2} &= \overline{\lambda}\frac{dN \wedge da}{|df|^2}\lambda + \frac{d(\overline{\lambda})N\lambda \wedge da}{|df|^2} - \frac{\overline{\overline{\lambda}Nd\lambda \wedge da}}{|df|^2} \\ &= \overline{\lambda}\frac{dN \wedge da}{|df|^2}\lambda + \frac{d(\overline{\lambda})N\lambda \wedge da}{|df|^2} - \frac{(d\overline{\lambda})\overline{\overline{\lambda}N} \wedge da}{|df|^2} \\ &= \overline{\lambda}\frac{dN \wedge da}{|df|^2}\lambda + \frac{d(\overline{\lambda})N\lambda \wedge da}{|df|^2} + \frac{(d\overline{\lambda})N\lambda \wedge da}{|df|^2} \\ &= \overline{\lambda}\frac{dN \wedge da}{|df|^2}\lambda + 2\frac{d\overline{\lambda} \wedge da}{|df|^2}N\lambda\,.\end{aligned}$$

The first term describes a similarity transformation in the tangent plane of the tangent-valued 0-form $\frac{dN \wedge da}{|df|^2}$, whereas the second term is a *differential* contribution in λ.
Further restricting to rigid deformations, where λ is a constant quaternionic function, we obtain

$$\frac{d\tilde{N} \wedge da}{|d\tilde{f}|^2} = \overline{\lambda}\frac{dN \wedge da}{|df|^2}\lambda\,,$$

which is a global, rigid similarity transformation.

6.3 Eigensolutions over $\mathbb{H}$

In Chapters 6.1 and 6.2, we have dealt with *real valued* functions and it is natural to ask how this framework extends to functions $\psi : M \to \mathbb{H}$. Being a normal operator on $L^2(M, \mathbb{H})$, $\mathcal{D}_f^2$ induces a *quaternionic* eigenbasis of $L^2(M, \mathbb{H})$, as outlined in Chapter 2.3. Consequently, it is tempting to infer geometric information from the eigensystem of $\mathcal{D}_f^2$ over $\mathbb{H}$. In analogy to the notion of *diffusion geometry* for the Laplace-Beltrami operator, we use the more general term *spectral geometry* for methods that aim to recover geometric information from the eigensystem of the Dirac operator.
However, it turns out that there is no canonical way of extracting geometric information from this eigensystem as we will show in the following. More precisely, for a quaternionic function in the decomposition Eq. (2.10),

$$\psi = a + \hat{Y} + bN, \tag{6.12}$$

there is no such geometrically meaningful decomposition of $\mathcal{D}_f^2\psi$. In particular we lose real part equivalence to the Laplace-Beltrami operator.

In the following, we analyze the contribution of the decomposition Eq. (6.12) to the second term in Eq. (6.1),

$$\frac{dN \wedge d\psi}{|df|^2}\,.$$

To this end, we use concepts and notation from classical Differential Geometry, which are introduced in the Appendix.

To begin with, the contribution from the *scalar part* of ψ is covered by Lemma 6.2. It is purely tangent-valued.
A closer analysis of the *tangent part* of ψ is given by the following lemma, which aims to isolate scalar, tangent and normal components in local coordinates.

Lemma 6.5. *Let X_1, X_2 be the principal curvature directions with associated principal curvatures κ_1, κ_2. Then,*

$$\begin{aligned} dN \wedge d\hat{Y}(X_1, X_2) = &\underbrace{\kappa_2 g(X_2, \nabla_{X_1} Y) - \kappa_1 g(X_1, \nabla_{X_2} Y)}_{\textit{scalar}} \\ &+ \underbrace{\kappa_1\kappa_2 (g(X_1, Y)\hat{X}_1 - g(X_2, Y)\hat{X}_2)}_{\textit{tangent}} \\ &+ \underbrace{(\kappa_1 \hat{X}_1 \times df(\nabla_{X_2} Y) - \kappa_2 \hat{X}_2 \times df(\nabla_{X_1} Y)}_{\textit{normal}} . \end{aligned} \tag{6.13}$$

In particular, $\frac{dN \wedge d\hat{Y}}{|df|^2}$ has scalar, tangent and normal contribution.

Proof. We have the freedom to choose local coordinates on M. As it is always helpful to choose an orthonormal coordinate system with geometric meaning, let X_1, X_2 be the principal curvature directions with associated principal curvatures κ_1, κ_2. By definition of the wedge product,

$$\begin{aligned} dN \wedge d\hat{Y}(X_1, X_2) &= dN(X_1) d\hat{Y}(X_2) - dN(X_2) d\hat{Y}(X_1) \\ &= \kappa_1 df(X_1) d\hat{Y}(X_2) - \kappa_2 df(X_2) d\hat{Y}(X_1). \end{aligned}$$

We can further specify each term as

$$\begin{aligned} df(X_1) d\hat{Y}(X_2) &= \hat{X}_1 \hat{\nabla}_{\hat{X}_2} \hat{Y} \\ &= \hat{X}_1 \Big(df(\nabla_{X_2} Y) + II(X_2, Y) N \Big) \\ &= \hat{X}_1 \Big(df(\nabla_{X_2} Y) + g(SX_2, Y) N \Big) \\ &= \hat{X}_1 df(\nabla_{X_2} Y) + \kappa_2 g(X_2, Y) \hat{X}_1 N. \end{aligned}$$

As all push-forwards are tangent-valued, using the definition of the Hamilton product (Eq. (2.4)) and the relations $\langle \hat{X}_i, N \rangle = 0$, $\hat{X}_i \times N = -\hat{X}_j$ for $i, j \in \{1, 2\}$, $i \neq j$, we arrive at

$$df(X_1) d\hat{Y}(X_2) = -\langle \hat{X}_1, df(\nabla_{X_2} Y) \rangle + \hat{X}_1 \times df(\nabla_{X_2} Y) - \kappa_2 g(X_2, Y) \hat{X}_2 .$$

Altogether,

$$\begin{aligned} dN \wedge d\hat{Y}(X_1, X_2) = &\underbrace{\kappa_2 g(X_2, \nabla_{X_1} Y) - \kappa_1 g(X_1, \nabla_{X_2} Y)}_{\text{scalar}} \\ &+ \underbrace{\kappa_1\kappa_2 (g(X_1, Y)\hat{X}_1 - g(X_2, Y)\hat{X}_2)}_{\text{tangent}} \\ &+ \underbrace{(\kappa_1 \hat{X}_1 \times df(\nabla_{X_2} Y) - \kappa_2 \hat{X}_2 \times df(\nabla_{X_1} Y)}_{\text{normal}} . \end{aligned}$$

□

The *normal part* of ψ yields a decomposition as stated in the following lemma.

Lemma 6.6. *Let N be the Gauss map of an oriented immersed surface $f : M \to \mathbb{R}^3$, $b : M \to \mathbb{R}$ and κ the Gaussian curvature, then*

$$\frac{dN \wedge d(bN)}{|df|^2} = \frac{dN \wedge db}{|df|^2} N + 2b\kappa N, \tag{6.14}$$

where $(dN \wedge db)N$ is tangent-valued and $2b\kappa N$ is normal valued.

Proof. Let X_1, X_2 be the principal curvature directions. Then

$$\begin{aligned} dN \wedge d(bN)(X_1, X_2) &= dN \wedge [(db)N + b\, dN](X_1, X_2) \\ &= dN \wedge (db)N(X_1, X_2) + (dN \wedge dN)b(X_1, X_2) \\ &= [dN \wedge db(X_1, X_2)]N + 2b\kappa N , \end{aligned}$$

where in the last line we used that $dN(X_i)dN(X_j) = dN(X_i) \times dN(X_j)$ for $i, j \in \{1, 2\}$, $i \neq j$, from which we can deduce that

$$\begin{aligned} dN \wedge dN(X_1, X_2) &= dN(X_1)dN(X_2) - dN(X_2)dN(X_1) \\ &= 2dN(X_1)dN(X_2) \\ &= 2\kappa_1\kappa_2 df(X_1)df(X_2) \\ &= 2\kappa(df(X_1) \times df(X_2)) \\ &= 2\kappa N . \end{aligned}$$

By Lemma 6.2, $dN \wedge db(X_1, X_2)$ is tangent-valued and for every tangent vector t, the Hamilton product $tN = -\langle t, N\rangle + t \times N = t \times N$ is tangent-valued. It follows that $\frac{dN \wedge dbN}{|df|^2}$ is tangent-valued. □

Finally, to draw a conclusion for the overall decomposition of $\mathcal{D}_f^2$, it is necessary to discuss the expression

$$\Delta_{g_f}\mathrm{Im}(\psi)\,.$$

The term $\Delta_{g_f}\psi$ for a quaternion-valued function ψ is meant as the *vector* Laplace-Beltrami operator, that is, the Laplace-Beltrami operator acting on every component of ψ as on a real valued function. It follows from this notational observation that $\Delta_{g_f}\psi \in \mathrm{Im}(\mathbb{H})$.

To summarize this discussion, the results for the squared Dirac operator acting on real valued functions do not generalize to the action on quaternion-valued functions, as in conclusion, the decomposition

$$D_f^2\psi = c + df(Z) + eN\,, \tag{6.15}$$

for real valued functions $c, e : M \to \mathbb{R}$, a vector field $Z \in TM$ and the normal map N, does *not* encode extractable geometric meaning.

In particular, the relation to the Laplace-Beltrami operator is lost in the sense that

$$\mathrm{Re}(\mathcal{D}_f^2\phi) \neq \Delta_{g_f}\mathrm{Re}(\phi)\,,$$

since there is an additional contribution as stated in Lemma 6.5.

This result has its analog for the discretized squared Dirac operator as derived in the proof of Lemma 6.5. It can be formally decomposed as

$$\begin{aligned}
(D^*D\phi)_i &= \sum_{j=1}^{|V|}(D^*D)_{ij}\phi_j \\
&= \sum_{j=1}^{|V|}(\mathrm{Re}((D^*D)_{ij}) + \mathrm{Im}((D^*D)_{ij}))(\phi_j^{(s)} + \phi_j^{(v)}) \\
&= \underbrace{\sum_{j=1}^{|V|}\mathrm{Re}((D^*D)_{ij})\phi_j^{(s)} - \left\langle \mathrm{Im}((D^*D)_{ij}), \phi_j^{(v)}\right\rangle}_{\text{real part}} \\
&\quad + \underbrace{\sum_{j=1}^{|V|}\mathrm{Re}((D^*D)_{ij})\phi_j^{(v)} + \mathrm{Im}((D^*D)_{ij}) \times \phi_j^{(v)} + \mathrm{Im}((D^*D)_{ij})\phi_j^{(s)}}_{\text{imaginary part}}\,.
\end{aligned} \tag{6.16}$$

More precisely, we can derive the imaginary part of the discretized squared Dirac operator from Eq. (6.8) together with Eq. (6.9), which for neighboring vertices $i \neq j$ with adjacent faces k_1, k_2 is given by

$$\mathrm{Im}((D^*D)_{ij}) = -\frac{1}{2A^{\mathrm{Voronoi}}}(N_{k_1} - N_{k_2})\,. \tag{6.17}$$

This term corresponds to a *tangent-valued* vector on the surface. As D^*D is a hermitian matrix the imaginary part of the diagonal is zero.
Consequently, for a given input vector $\phi \in \mathbb{H}^{|V|}$, besides the Laplace-Beltrami contribution, the tangent part of $\phi^{(v)}$ contributes to $\mathrm{Re}(D^*D\phi)$. This observation is in accordance with the continuous case made explicit in Lemma 6.5.

To conclude, it does not seem possible to construct a meaningful spectral geometry for the squared Dirac operator over $\mathbb{H}$.

6.4 Numerical demonstration

In the following, we demonstrate the relation of the Laplace-Beltrami operator and the squared Dirac operator numerically. As a deviation measure, we take the relative error

$$\frac{\mathrm{Re}(\mathcal{D}_f^2\phi) - \Delta_{g_f}\mathrm{Re}(\phi)}{\Delta_{g_f}\mathrm{Re}(\phi)}\,. \tag{6.18}$$

To this end, we apply the operators to smooth functions[22] that are of the same order of magnitude 10^0. For real valued ϕ, relation Eq. (6.4) is correct up to a numerical zero in the deviation measure Eq. (6.18) (order of magnitude 10^{-12}). The deviation when ϕ is a full quaternionic function is demonstrated in Fig 6.3. This figure illustrates two effects. First, the relative error is up to one order of magnitude larger than the input function, namely of magnitude 10^1. Secondly, the error does not correlate with any geometric features of the shape.

[22] slowly varying in the computational setup, e.g. Laplace-Beltrami eigenfunctions

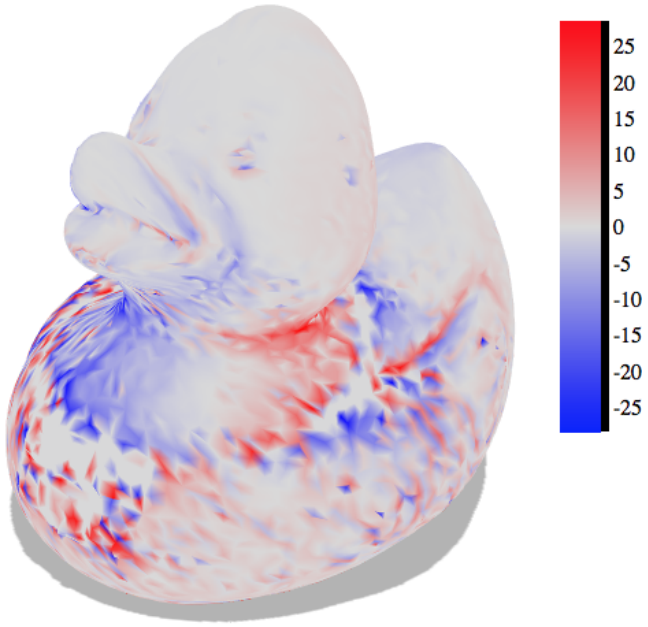

Figure 6.3: Relative error $\frac{\mathrm{Re}(\mathcal{D}_f^2\phi)-\Delta_{g_f}\mathrm{Re}(\phi)}{\Delta_{g_f}\mathrm{Re}(\phi)}$ for a smooth function $\phi : M \to \mathbb{H}$ with order of magnitude 10^0. To avoid scale distortion due to numerical errors, the 95th percentile of the absolute data values is displayed.

Chapter 7

As isometric as possible spin transformation

In this section we want to discuss the following problem: given a desired curvature potential ρ, determine an *as isometric as possible* λ-spin transformation while remaining *as close as possible* to ρ. In mathematical notation, we are looking for a $(\lambda^{(i)}, \rho^{(i)})$-spin transformation[23], such that $|\lambda^{(i)}|(p) \approx 1 \; \forall p \in M$ and $\mathrm{dist}(\rho, \rho^{(i)})$ is small for a suitable distance measure.
A possible application is a *sequence* of spin transformations along an *isometric path* in conformal shape space, which would be the first step to guide spin transformations along a path of *physical deformations*. Whereas isometries are not restrictive enough for physical deformations, it is also possible to control the extrinsic geometry via the curvature potential. The goal of this approach then is to control the overall deformation of the *shape* of a physical object guided by prescribing the curvature potential.
An approach for controlling intrinsic and extrinsic geometry for physical deformations that comes closest to this idea is carried out in [16] via a moving frame formulation. The authors are looking for an isometric deformation, which minimizes changes in the second fundamental form, i.e. minimizes distortion.

7.1 Isometric spin transformation and the notion of ρ-validity

Suppose we have an initial λ-spin transformation that satisfies the integrability condition Eq. (4.5) for a $\gamma = 0$ eigenvalue[24]. An equivalent representation is obtained in the form

$$E\lambda = 0 \qquad \Longleftrightarrow \qquad (EM)(M^{-1}\lambda) = 0\,, \tag{7.1}$$

for a suitable invertible matrix $M \in GL(|V|, \mathbb{H})$, where $E^{(i)} := EM$ should represent a transformation of some curvature potential $\rho^{(i)}$ and $\lambda^{(i)} := M^{-1}\lambda$ should be close to an isometric spin transformation.

[23] The superscript (i) stands for *isometric*.
[24] This assumption can be dropped while the argument remains valid by using the matrix $\tilde{E} := (E - \gamma \mathbf{1})$.

The easiest way to ensure such an isometric spin transformation based on an initial λ-spin transformation is to rescale each quaternion by its inverse norm, i.e.

$$\lambda^{(i)} = M^{-1}\lambda,$$

for $M \in \mathbb{H}^{|V|\times|V|}$ diagonal with $M_{ii} = |\lambda_i|$.
It turns out that this approach is too simple-minded. To work this out, we introduce the notion of *ρ-validity*.

Definition 7.1. *A transformation matrix E that can be derived from a curvature potential ρ by Eq.* (4.5),

$$E_{ij} = \sum_{k\in\{k_1,k_2\}} -\frac{e_i^{(k)} e_j^{(k)}}{4A_k} + \frac{1}{6}(\rho_i e_j^{(k)} - \rho_j e_i^{(k)}) + \frac{A_k}{9}\rho_i\rho_j\,, \tag{7.2}$$

is called ρ-valid.

Suppose $E \in \mathbb{H}^{|V|\times|V|}$ is the given initial transformation matrix that admits a solution $E\lambda = 0$. A necessary condition for $E^{(i)}$ to be ρ-valid is that it has to be hermitian, as we can see by Eq. (7.2), which leads to an element-wise comparison

$$\begin{aligned}
&(EM)^\dagger_{ij} = (EM)_{ij} \\
\Leftrightarrow\ &\sum_{k=1}^{|V|} M^\dagger_{ik} E^\dagger_{kj} = \sum_{k=1}^{|V|} E_{ik} M_{kj} \\
\Leftrightarrow\ &[\mathrm{Re}(E_{ji}) - \mathrm{Im}(E_{ji})]M_{ii} = [\mathrm{Re}(E_{ij}) + \mathrm{Im}(E_{ij})]M_{jj}
\end{aligned}$$

For a quaternionic hermitian matrix, $\mathrm{Re}(E_{ji}) = \mathrm{Re}(E_{ij}), \mathrm{Im}(E_{ji}) = -\mathrm{Im}(E_{ij})$ and for equality to hold, it follows that $M_{ii} = M_{jj}\ \forall i, j \in \{1, \ldots, |V|\}$. This corresponds to the case that M represents a *global scaling*. As a consequence, E cannot be transformed into a ρ-valid transformation matrix by non-global scaling.
We therefore need to closer analyze what it means for a matrix E to be *ρ-valid*.

7.2 Hermitian relaxation of ρ-validity

We start by formulating this problem with a weaker condition than ρ-validity, namely hermiticity. Every ρ-valid matrix is hermitian, but not every hermitian matrix is ρ-valid, as Eq. (7.2) imposes additional structural constraints. A sufficient condition for EM to be hermitian is that

- M is hermitian
- $EM = ME$

In summary, the hermitian relaxation of finding an isometric as possible spin transformation can be formulated as

$$\begin{aligned} \underset{M\in GL(|V|,\mathbb{H})}{\text{minimize}} \quad & \| |M^{-1}\lambda|_{\text{el}} - \mathbf{1}\|_2 \\ \text{subject to} \quad & M \text{ hermitian} \\ & ME - EM = 0\,, \end{aligned} \tag{7.3}$$

where we denote by $\mathbf{1} \in \mathbb{H}^{|V|}$ the vector with the real entries 1 and the *element-wise* norm[25] by $|\cdot|_{\text{el}}$, that is, for $\lambda \in \mathbb{H}^n$,

$$|\lambda|_{\text{el}} := (|\lambda_1|, |\lambda_2|, \ldots, |\lambda_n|) \in \mathbb{H}^n\,.$$

As the inverse of a hermitian matrix is hermitian, by introducing $A := M^{-1}$, the constraints can be equivalently formulated for a matrix A to obtain

$$\begin{aligned} \underset{A\in GL(|V|,\mathbb{H})}{\text{minimize}} \quad & \| |A\lambda|_{\text{el}} - \mathbf{1}\|_2 \\ \text{subject to} \quad & A \text{ hermitian} \\ & E^{-1}A - AE^{-1} = 0\,. \end{aligned} \tag{7.4}$$

The feasible set of this optimization problem is non-empty, as the quaternionic identity matrix satisfies the constraints.

To formulate the real representation of problem (7.4), we overload our notation and define the element-wise norm for $\boldsymbol{\phi} \in \mathbb{R}^{4|V|}$ as

$$|\boldsymbol{\phi}|_{\text{el}} := (||(\boldsymbol{\phi}_{11}, \boldsymbol{\phi}_{12}, \boldsymbol{\phi}_{13}, \boldsymbol{\phi}_{14})||_2, \ldots, ||(\boldsymbol{\phi}_{n1}, \boldsymbol{\phi}_{n2}, \boldsymbol{\phi}_{n3}, \boldsymbol{\phi}_{n4})||_2) \in \mathbb{R}^{|V|},$$

and use the symbol $\mathbf{1} \in \mathbb{R}^{|V|}$ for the vector with all entries equal to 1.
As outlined in Chapter 4.1, a quaternionic matrix A is hermitian, if and only if its real representation $\boldsymbol{A}$ is symmetric. Therefore, the equivalent real optimization problem reads

$$\begin{aligned} \underset{\boldsymbol{A}\in GL(4|V|,\mathbb{R})}{\text{minimize}} \quad & \| |\boldsymbol{A\lambda}|_{\text{el}} - \mathbf{1}\|_2 \\ \text{subject to} \quad & \boldsymbol{A} \text{ symmetric} \\ & \boldsymbol{E}^{-1}\boldsymbol{A} - \boldsymbol{A}\boldsymbol{E}^{-1} = 0. \end{aligned} \tag{7.5}$$

Unfortunately, this optimization problem requires working with a difficult objective function. Optimization problems in the context of isometric spin transformations naturally involve a formulation on $\prod^{|V|}\mathbb{S}^3$, the $|V|$-fold product of the unit sphere in $\mathbb{R}^4$.

[25] which obviously is not a norm in the usual sense, as it does not map into the non-negative reals

7.3 Recovering the curvature potential from a ρ-valid transformation matrix

After modifying the transformation matrix according to Eq. (7.1) as $E^{(i)} := EM$, it is necessary to solve the inverse problem of recovering the curvature potential $\rho^{(i)}$ from $E^{(i)}$.
This leads to solving a *non-linear* system of equations. Rearranging Eq. (7.2) leads to $|V|^2$ non-linear *quaternion* equations of the form[26]

$$\sum_{k\in\{k_1,k_2\}} -\frac{e_i^{(k)} e_j^{(k)}}{4A_k} + \frac{1}{6}(\rho_i e_j^{(k)} - \rho_j e_i^{(k)}) + \frac{A_k}{9}\rho_i\rho_j - E_{ij} = 0.$$

Its discrete representation yields $(4|V|)^2$ non-linear *real* equations to determine $|V|$ real values of $(\rho_i)_{i=1}^{|V|}$. This problem can be numerically solved using the `fsolve` MATLAB routine.

7.4 Algorithmic pipeline

The method to achieve an as isometric as possible spin transformation while controlling the mean curvature via the curvature potential can be outlined as follows:

1. Start with an initial (λ, ρ)-spin transformation.
2. Determine the matrices M that lead to $\rho^{(i)}$-valid transformation matrices EM, while transforming λ into a nearly isometric deformation via $\lambda^{(i)} = M^{-1}\lambda$.
3. Solve the inverse problem for the corresponding curvature potential $\rho^{(i)}$ as described in Chapter 7.3.
4. Select a specific M among all possible ones, which yields a desired trade-off between $\rho^{(i)}$ and $\lambda^{(i)}$.

In summary, we have outlined a possibility to interact with the spin transformation process in order to obtain an as isometric as possible spin transformation. Even though the hermitian relaxation already leads to a difficult optimization problem, it remains an additional challenge to advance beyond the hermitian relaxation of ρ-validity and specify necessary and sufficient conditions for ρ-validity via Eq. (7.2).

[26] The superscript (i) is dropped to reduce the notational complexity.

Chapter 8

Summary, conclusion and outlook

Quaternionic Shape Analysis provides a theoretically profound and practically feasible framework for conformal deformations of shapes and incorporates the intrinsic and extrinsic geometry. We have proposed ideas to tackle the problem of considering a special subclass of conformal deformations, namely that of isometries. Whereas common approaches use *only* this intrinsic geometry to describe *physical deformations*, we have motivated that in fact the extrinsic geometry is useful when dealing with physical deformations and necessary to uniquely determine a *shape* from a theoretical point of view. This motivation strongly suggests that examining the class of isometries within Quaternionic Shape Analysis is a valuable viewpoint.

We demonstrated that prevalent diffusion geometric ideas can be recovered within Quaternionic Shape Analysis, such that it offers a *superset* of methods. More precisely, the action of the Laplace-Beltrami operator can be expressed by using the squared Dirac operator. Our Theorem 6.4 shows that this relation induces the common cotangent weight Laplacian as a discretization for the Laplace-Beltrami operator. This directly implies that the discretization outlined for the Dirac operator in Chapter 4.2 can be used to *compute* all methods using Laplace-Beltrami diffusion geometry. It can be viewed as a consistency result for the discretization via the Finite Element method.
We investigated how the idea of Laplace-Beltrami diffusion geometry generalizes to a spectral geometry of the squared Dirac operator over $\mathbb{H}$. Our results show that there is no canonical way to extend the framework of real valued functions to full quaternions, in particular we proved that the relation to the Laplace-Beltrami operator is lost.
Besides these spectral geometric notions, central quantities and operators of Differential Geometry can be related to the Dirac operator. Along the idea of establishing a unified framework, it is therefore an interesting problem to investigate the properties of their discretization as *directly derived* from the discrete Dirac operator as it has been carried out for the Laplace-Beltrami operator in this thesis.

The central idea behind Laplace-Beltrami diffusion geometry is to use invariance of the eigenvalue problem under isometric deformation. As the Dirac operator analogously induces an eigenbasis on

a quaternionic L^2 Hilbert space, this procedure led us to investigate how the eigenvalue problem of the Dirac operator changes under the natural transformation within Quaternionic Shape Analysis, namely spin transformation. Our Theorem 5.1 describes this change and reveals a surprisingly simple result, which has a geometric interpretation. As a first application, we attempted to recover information about spin transformation between two shapes only from their Dirac operators. However, a more detailed investigation disclosed that this approach would not yield a superior method to working directly with spin transformation and the integrability condition. Nevertheless, the statement of Theorem 5.1 is at the heart of relating shapes via spectral geometric ideas and might well play a role in future research efforts.

As a direct formulation of specifying the class of isometries within the class of conformal deformations, we outlined a pipeline for *as isometric as possible* spin transformations, which are guided by an *extrinsic* geometric measure, the curvature potential. To formulate this point of view, we introduced the notion of ρ-validity, a structural condition on the matrices, which govern a spin transformation. Such matrices are necessarily hermitian, which led us to first investigate the weaker hermiticity relaxation of ρ-validity. However, already formulating this hermitian relaxation leads to a difficult optimization problem. In general, optimization problems related to isometric spin transformations involve the product of unit spheres in $\mathbb{R}^4$. Obtaining a feasible formulation of this class of optimization problems is necessary to solve inverse problems within isometric Quaternionic Shape Analysis. Besides the optimization formulation, the structural problem of finding necessary and sufficient conditions for ρ-validity is at the core of any feedback mechanism from λ to ρ and will continue to receive attention in future research.
The investigation of both of these problems will help to better understand isometric deformations within the framework.

We used the Finite Element paradigm for discretization in this thesis and were able to successfully recover the cotangent Laplacian via the squared Dirac operator. A fruitful research direction would be to investigate the discretization with the alternative approach of *Discrete Exterior Calculus*, which has recently received considerable attention (cf. [5], [12]).

Naturally in our approach, isometric spin transformations are covered by setting $|\lambda| \equiv 1$ in a more general computation. To devise a *robust* algorithmic method, it is an important open problem how these results behave under a *perturbation* from isometry, as in any discrete model one can only hope for *near* isometries.

Recently, methods of Shape Analysis and Geometry Processing were combined in [2] to construct shape analogies. The approach is based on the intrinsic geometry as encoded by the Laplace-Beltrami operator and the extrinsic geometry enters as an initial shape of the optimization algorithm. In future research, it would be an interesting application of the framework to investigate

how this problem can be formulated within Quaternionic Shape Analysis, which could potentially provide a stronger connection to the extrinsic geometry and thus to the overall *shape*.

In conclusion, the Quaternionic Shape Analysis framework has the potential to provide a holistic paradigm within which common task of Shape Analysis can be formulated and important quantities can be extracted. This statement includes the intrinsic and the extrinsic surface geometry. Purely intrinsic methods can be recovered and complemented by extrinsic methods. This scope justifies the computational overhead, in particular an increased memory use for the storage of quaternions. The ideas and open questions developed in this thesis provide a promising starting point for future research towards a unified framework for Shape Analysis.

Appendix

Differential Geometry of surfaces

In this appendix we introduce some notions of the Differential Geometry of surfaces, which are used throughout the thesis. A more detailed discussion can be be found in [8] and [15].

We consider 2-dimensional surfaces immersed into $\mathbb{R}^3$, where an *immersion* is a differentiable function $f : M \to \mathbb{R}^3$, from a topological surface[27] M to Euclidean space $\mathbb{R}^3$, whose derivative is everywhere injective. Phrased differently, at every point $p \in M$, the Jacobian of the mapping f in local coordinates has rank two, i.e. there are two linearly independent column vectors. Geometrically speaking, one can place a plane at every point of the surface that is spanned by the column vectors of the Jacobian. This plane is called *tangent plane* to M at p, which is denoted by T_pM. The collection of these tangent planes is the *tangent bundle* $TM := \bigcup_{p\in M}\{p\} \times \{T_pM\}$.
The differential of an immersion is a linear map $df : TM \to T\mathbb{R}^3 = \mathbb{R}^3$ between the tangent space of the abstract surface and its immersion into $\mathbb{R}^3$. In order to distinguish vector fields on M and in the ambient space $\mathbb{R}^3$, we will use a hat, i.e. for $X \in TM$, $\hat{X} := df(X)$. For this reason the differential is also called the push-forward of tangent vectors on M to the ambient space. In this thesis, we deal with *conformal* immersions, that is, the angle between vector fields on M is preserved by the push-forward to $\mathbb{R}^3$ as illustrated in Fig. 1.

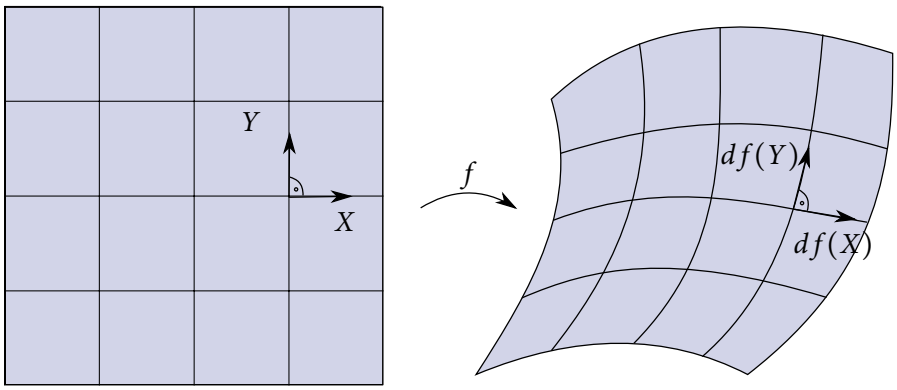

Figure 1: Illustration of a conformal immersion. The angle between vector fields X, Y is preserved by push-forward.

[27] A topological space that locally looks like (is homeomorphic to) the Euclidean plane.

It is important to note that we don't restrict ourself to special surfaces.

For a given topological surface M, *a conformal immersion always exists*.

This seems like an unreasonably strong statement at first sight, but here is the *construction* of such a conformal immersion:
Consider a complex structure $\mathcal{J}$ on M, that is, a map $\mathcal{J} : TM \to TM$ such that $\mathcal{J}^2 = -\mathrm{id}$. Intuitively, $\mathcal{J}$ represents a *counterclockwise* 90° *rotation* in tangent space.
An immersion f is conformal if $|df(X)| = |df(\mathcal{J}X)|$ and $\langle df(X), df(\mathcal{J}X)\rangle = 0$ for all vector fields X on M. Alternatively this can be characterized as

$$df(\mathcal{J}X) = N \times df(X) \quad \forall X \in TM\,, \tag{A.1}$$

where $N : M \to \mathbb{S}^2 \subset \mathbb{R}^3$ is the oriented unit normal field, also called *Gauss map*. For every point $p \in M$, N_p is the unit vector orthogonal to the tangent plane T_pM pointing outward.
Eq. (A.1) *uniquely* determines $\mathcal{J}$: For a given $X \in TM$ define $\mathcal{J}X$ as the vector field satisfying (A.1), then

$$df(\mathcal{J}^2X) = N \times df(\mathcal{J}X) = N \times (N \times df(X)) = df(-X), \tag{A.2}$$

As the differential of an immersion is by definition injective, $\mathcal{J}X$ is uniquely defined. Thus, $\mathcal{J}$ is a complex structure that makes f a conformal immersion. However, this does not imply that all immersions are *conformally equivalent*.
With local coordinates (x_1, x_2), we can formulate a *moving frame* description of an immersed surface, by describing vector fields on the immersed surface in a basis $\{f_{x_1}, f_{x_2}, N\}$, where the partial derivatives $\{f_{x_1}, f_{x_2}\}$ form a basis of the tangent plane and N is the normal direction. This means that the decomposition of a vector in tangent and normal component *varies* over the surface.
Most immersions appearing in this thesis are of a special type, namely *embeddings*, i.e. f is in addition an homeomorphism[28] onto $f(M)$.
Let us consider an example in $\mathbb{R}^2$ for the property we should have in mind when dealing with embeddings. Consider the sketches in Fig. 2. The immersion of a real interval $M = [0, 1)$ on the right side is *not* an embedding as the pre-image of the intersection point consists of two points in M and therefore the immersion is not injective. The take-home message: embeddings do *not* have intersections.

[28] a bijective, continuous function between topological spaces with continuous inverse function

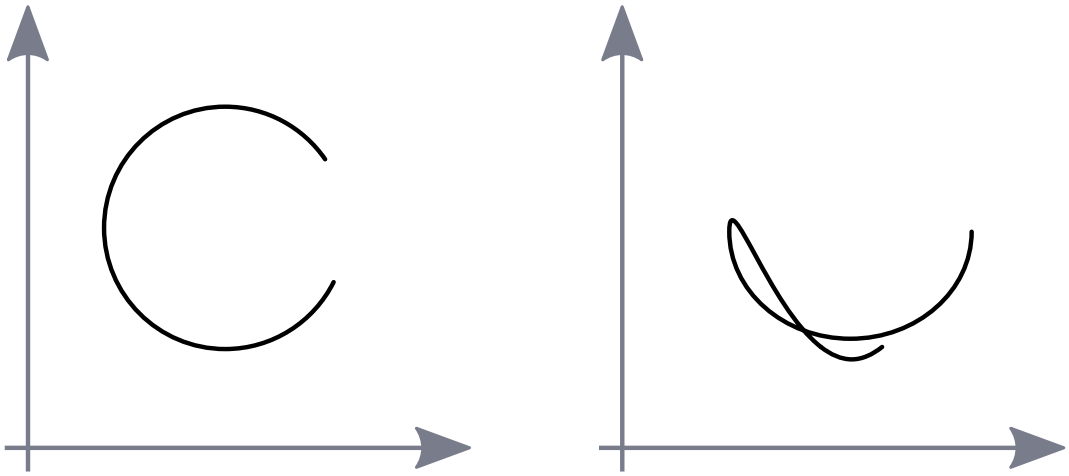

Figure 2: Comparison of an immersion (both) with an embedding (left) for the topological space $M = [0,1)$ into $\mathbb{R}^2$. An embedding is *intersection-free*.

The surfaces M appearing in this thesis are compact, simply connected and orientable. The *Riemannian metric* or *first fundamental form* on M is defined as

$$g(X,Y) := \langle df(X), df(Y) \rangle ,$$

for all vector fields $X, Y \in TM$ with the standard inner product $\langle \cdot, \cdot \rangle$ on $\mathbb{R}^3$. It is a quadratic form and as such can be expressed via a matrix in local coordinates (x_1, x_2). Suppose a surface patch can be described by a local parametrization $f(x_1, x_2)$ around some point $p \in M$. The partial derivatives (f_{x_1}, f_{x_2}) in coordinate directions form a basis of T_pM. For two vectors $w_1, w_2 \in T_pM$,

$$g(w_1, w_2) = w_1 \begin{pmatrix} E & F \\ F & G \end{pmatrix} w_2,$$

where the matrix coefficients are given by

$$\begin{aligned} E &= \langle f_{x_1}, f_{x_1} \rangle_p \\ F &= \langle f_{x_1}, f_{x_2} \rangle_p \\ G &= \langle f_{x_2}, f_{x_2} \rangle_p \end{aligned}$$

Note the dependence on $p \in M$. The coefficients are not constant, but they are smooth functions over the surface that depend on the parametrization.

The first fundamental form allows for *measurements* that are taken *on* the surface. It describes the *intrinsic* geometry of the surface by fixing distances *on* the surface. Two surfaces with the same Riemannian metric are called *isometric*. In fact, the outer appearance – or *shape* – of an object is not

determined by the intrinsic geometry alone, but the *extrinsic* geometry has to be taken into account.

The extrinsic geometry is described by the behavior of the Gauss map. The differential character of the Gauss map is captured by the *shape operator*[29] and, as a related concept, by the *second fundamental form*.
The shape operator is defined pointwise for $p \in M$ as

$$S_p : T_pM \to T_pM, w \mapsto -\hat{\nabla}_w N_p, \tag{A.3}$$

which is the negative directional derivative[30] of the normal map at point p in the direction of w. By definition, the shape operator relates to the differential of the Gauss map via

$$df(SX) = -dN(X) \qquad \forall X \in TM,$$

where the differential of the Gauss map $dN_p : T_pM \to T_pM$ is a pointwise defined, self-adjoint, linear map. We use the associated quadratic form to define the second fundamental form as

$$II(X, Y) := -\langle dN(X), df(Y)\rangle = g(SX, Y) \qquad X, Y \in TM. \tag{A.4}$$

For two tangent vectors $w_1, w_2 \in TM$, the matrix representation in local coordinates is expressed as

$$II(w_1, w_2) = w_1 \begin{pmatrix} l & m \\ m & n \end{pmatrix} w_2. \tag{A.5}$$

The *second order* differential quantities of the immersion are captured by the *Christoffel symbols*. Whereas the first derivatives (f_{x_1}, f_{x_2}) in a local parametrization (x_1, x_2) are tangent-valued, the second derivatives $(f_{x_1x_1}, f_{x_1x_2}, f_{x_2x_1}, f_{x_2x_2})$ also have a normal contribution. The Christoffel symbols $\mathbf{\Gamma}^k_{ij}$ $i, j, k \in \{1, 2\}$ are the coefficients of these functions in the basis $\{f_{x_1}, f_{x_2}, N\}$. More precisely,

$$\begin{aligned} f_{x_1x_1} &= \mathbf{\Gamma}^1_{11} f_{x_1} + \mathbf{\Gamma}^2_{11} f_{x_2} + lN \\ f_{x_1x_2} &= \mathbf{\Gamma}^1_{12} f_{x_1} + \mathbf{\Gamma}^2_{12} f_{x_2} + mN \\ f_{x_2x_1} &= \mathbf{\Gamma}^1_{21} f_{x_1} + \mathbf{\Gamma}^2_{21} f_{x_2} + mN \\ f_{x_2x_2} &= \mathbf{\Gamma}^1_{22} f_{x_1} + \mathbf{\Gamma}^2_{22} f_{x_2} + nN\,. \end{aligned} \tag{A.6}$$

The Christoffel symbols are smooth functions over the surface and depend on the intrinsic geometry only, that is, can be expressed in terms of the coefficients of the first fundamental form.
It is at this level of second order quantities, where the compatibility conditions of first and second fundamental form originate. As the immersion f is a smooth function, the second partial deriva-

[29] An alternative common name is *Weingarten map*.
[30] The notational choice of denoting the directional derivative by $\hat{\nabla}$ becomes clear later on in this section.

tives in local coordinates exchange by Schwarz' theorem, namely $(f_{x_1})_{x_2} = (f_{x_2})_{x_1}$. Starting with Eqs. (A.6), this requirement leads to the *Gauß-Mainardi-Codazzi equations*:

$$\begin{aligned} l_{x_2} - m_{x_1} &= l\Gamma^1_{12} + m(\Gamma^2_{12} - \Gamma^1_{11}) - n\Gamma^2_{11} \\ m_{x_2} - n_{x_1} &= l\Gamma^1_{22} + m(\Gamma^2_{22} - \Gamma^1_{12}) - n\Gamma^1_{12}\,. \end{aligned} \tag{A.7}$$

This coupled system of partial differential equations with variable coefficients Γ^k_{ij} defines which combination of first and second fundamental form lead to an integrable surface. Hence they are also called *integrability conditions*.

A central notion in a surface description is that of *curvature*. Consider a curve

$$\alpha : (-\varepsilon, \varepsilon) \to M, s \mapsto \alpha(s)$$

around a fixed point $\alpha(0) = p \in M$ on the surface as illustrated in Fig. 3. We denote the initial direction as $\alpha'(0) =: \hat{X}$, where $X \in TM$ is a unit vector field. The curvature of the curve is given by the second derivative[31]

$$\alpha'' = \underbrace{\alpha''_t}_{\text{tangent}} + \underbrace{\langle \alpha'', N \rangle N}_{\text{normal}} \tag{A.8}$$

Using integration by parts and the fact that the first derivative α' is purely tangential,

$$\left\langle \frac{d^2\alpha}{ds^2}, N \right\rangle N = -\left\langle \alpha', \frac{\partial N}{\partial s} \right\rangle N = -\left\langle \alpha', \hat{\nabla}_{\hat{X}} N \right\rangle N = g(X, SX)N = II(X, X)N.$$

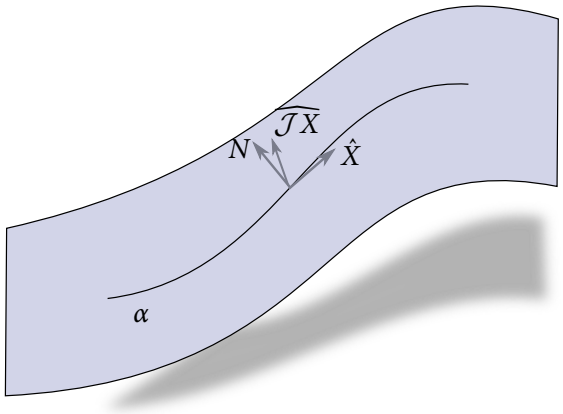

Figure 3: Illustration of a curve α on the surface M with initial direction $\alpha'(0) = \hat{X}$.

[31] $s \in (-\varepsilon, \varepsilon)$ can be considered as a time parameter with respect to which we take the derivative here.

This observation justifies the definition of *normal curvature* for all unit vector fields $X \in TM$ as

$$\kappa_N(X) := II(X, X). \tag{A.9}$$

Normal curvature has an intuitive geometric interpretation, which is demonstrated in Fig. 4. The normal curvature in direction $X \in TM$, is equal to the inverse radius of a disk that can be locally fitted to the surface in direction X.

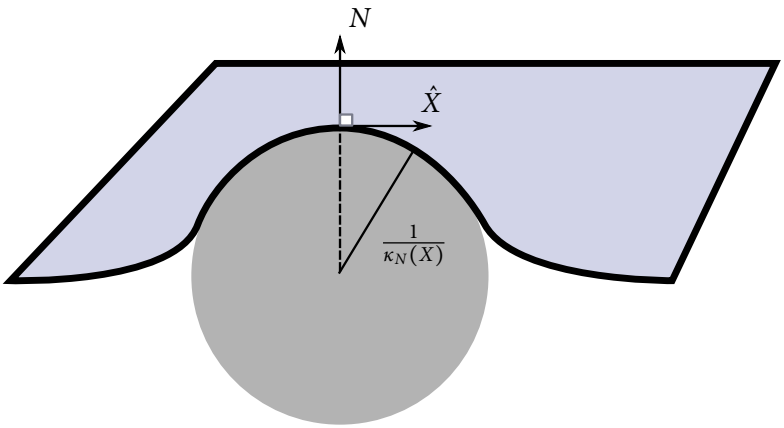

Figure 4: Illustration of normal curvature. Normal curvature $\kappa_N(X) = 1/R$ is equal to the inverse radius of a disk that can locally be fitted to the surface in direction of a vector field $X \in TM$.

The maximum and the minimum curvatures among all possible directions at a point $p \in M$ are the principal curvatures $\kappa_1(p), \kappa_2(p)$. Let X_1, X_2 be the corresponding (unit norm) directions of principal curvature. These are the eigenvectors of the shape operator with eigenvalues κ_1, κ_2, respectively,

$$SX_i = \kappa_i X_i. \tag{A.10}$$

As a consequence, the differential of the Gauss map evaluated along the principal curvature directions is

$$dN(X_i) = \kappa_i df(X_i). \tag{A.11}$$

The Gaussian curvature κ and mean curvature H of a surface are defined as

$$\begin{aligned} \kappa &= \kappa_1 \kappa_2 \\ H &= \frac{\kappa_1 + \kappa_2}{2}. \end{aligned} \tag{A.12}$$

By Gauß' *Theorema Egregium*, the Gaussian curvature depends only on the intrinsic geometry. Mean curvature on the other hand is an extrinsic curvature measure.

Since the point of view taken in this thesis is based on differential quantities of the surface, we need a notion of derivative *as seen from the surface* called the *covariant derivative*.

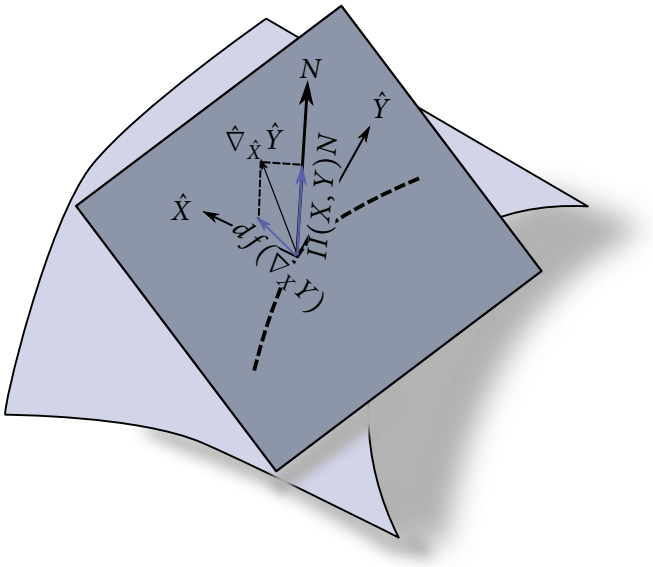

Figure 5: Illustration of the covariant derivative, which is the tangential component of the directional derivative in ambient space.

Let $\hat{X} = df(X)$, $\hat{Y} = df(Y)$ be vector fields in $\mathbb{R}^3$ associated with $X, Y \in TM$ via push-forward. We denote the directional derivative of $\hat{Y}$ in direction $\hat{X}$ in Euclidean space by[32]

$$\hat{\nabla}_{\hat{X}}\hat{Y}\,.$$

This expression has tangential and normal contribution. The idea of the *covariant derivative* is to project the directional derivative onto the tangent bundle of the surface M. It can be written as $df(\nabla_X Y)$, where ∇ is the Levi-Civita connection on M.
Altogether, we have the decomposition

$$\hat{\nabla}_{\hat{X}}\hat{Y} = \underbrace{df(\nabla_X Y)}_{\text{tangent}} + \underbrace{II(X,Y)N}_{\text{normal}}\,. \tag{A.13}$$

[32]The directional derivative in Euclidean space is the Levi-Civita connection, which makes this choice of notation clear.

Nomenclature

$\lvert q\rvert$	norm of a quaternion $q \in \mathbb{H}$
α, β	generic quaternionic differential forms
A^*	mesh adjoint of a matrix A
$\langle \cdot, \cdot \rangle_{\mathfrak{H}}$	inner product on a Hilbert space $\mathfrak{H} \in \{\mathbb{R}^n, \mathbb{H}^n, L^2(M, \mathbb{R}), L^2(M, \mathbb{H})\}$; if the Hilbert space is clear from context, it is not specified explicitly
$Q^\dagger$	hermitian adjoint of a quaternionic matrix, that is, Q transposed and conjugated
Δ_{g_f}	Laplace-Beltrami operator to the metric g associated with the surface immersed by f
df	differential of the immersion f
$\lvert df\rvert^2$	volume form of a conformal immersion $f : M \to \mathbb{R}^3$
$\frac{1}{\lvert df\rvert^2}$	Hodge star operator on 2-forms
$\mathcal{D}_f$	quaternionic Dirac operator to a conformal immersion $f : M \to \mathbb{R}^3$
F	face set of the surface mesh with $\lvert F\rvert$ faces
f	immersion of a surface M into $\mathbb{R}^3$
f_x	partial derivative of the immersion $f : M \to \mathbb{R}^3$ with respect to x
g	Riemannian metric
$\mathbf{\Gamma}_{ij}^k$	Christoffel symbols
$\mathbb{H}$	quaternion skew-field
$\mathcal{H}$	inner product space of half-densities
H	mean curvature
$\wedge$	wedge product between differential forms
$H\lvert df\rvert$	mean curvature half-density

$I(X, Y)$ first fundamental form evaluated at vector fields X, Y

$II(X, Y)$ second fundamental form evaluated at vector fields X, Y

$\mathrm{Im}(q)$ imaginary part of a quaternion $q \in \mathbb{H}$

$\mathcal{J}$ complex structure on a surface

κ Gaussian curvature

κ_1, κ_2 principal curvatures along principal curvature directions X_1, X_2

λ quaternionic function $\lambda : M \to \mathbb{H} \setminus \{0\}$ that induces a spin transformation

M domain of immersion (topological surface)

$\mathcal{M}_f$ conformal shape space based on the immersion $f : M \to \mathbb{R}^3$

N outward oriented normal field (Gauss map)

$\hat{\nabla}_{\hat{X}} \hat{Y}$ covariant derivative in ambient space of a tangent vector field $\hat{Y}$ in direction $\hat{X}$

$\nabla_X Y$ Levi-Civita connection on a surface M with vector fields X, Y on M as arguments

$\Omega_k(M)$ space of differential k-forms on a surface M

ω, η generic real valued differential forms

ϕ, ψ generic functions

$\overline{q}$ conjugated quaternion to a quaternion $q \in \mathbb{H}$

$q^{(s)}$ scalar part of a quaternion $q \in \mathbb{H}$

$q^{(v)}$ vector part of a quaternion $q \in \mathbb{H}$

$\mathrm{Re}(q)$ real part of a quaternion $q \in \mathbb{H}$

ρ curvature potential

S shape operator

σ volume form

$\star$ Hodge star operator

TM tangent bundle over the surface M

u, v, w generic vectors

V vertex set of the surface mesh with $|V|$ vertices

$\times$	cross product in $\mathbb{R}^3$
x_i	local coordinates on M
X, Y	generic vector fields on a surface
$\hat{X}, \hat{Y}$	push-forwards of vector fields X, Y on a surface to the ambient space

Bibliography

[1] Mathieu Aubry, Ulrich Schlickewei, and Daniel Cremers. The Wave Kernel Signature: A Quantum Mechanical Approach to Shape Analysis. In *Computer Vision Workshops (ICCV Workshops), 2011 IEEE International Conference on*, pages 1626–1633, 2011.

[2] Davide Boscaini, Davide Eynard, and Michael M. Bronstein. Shape-from-intrinsic operator. Technical Report arXiv:1406.1925, 2014.

[3] Alexander Bronstein, Michael Bronstein, and Ron Kimmel. *Numerical Geometry of Non-Rigid Shapes*. Springer, 2008.

[4] Keenan Crane. *Conformal Geometry Processing*. PhD thesis, Calfornia Institute of Technology, 2013.

[5] Keenan Crane, Fernando de Goes, Mathieu Desbrun, and Peter Schröder. Digital Geometry Processing with Discrete Exterior Calculus. In *ACM SIGGRAPH 2013 Courses*, SIGGRAPH '13, pages 7:1–7:126, 2013.

[6] Keenan Crane, Ulrich Pinkall, and Peter Schröder. Spin Transformations of Discrete Surfaces. *ACM Trans. Graph.*, 30(4):104:1–104:10, 2011.

[7] Mathieu Desbrun, Mark Meyer, Peter Schröder, and Alan H. Barr. Implicit Fairing of Irregular Meshes Using Diffusion and Curvature Flow. In *Proceedings of the 26th Annual Conference on Computer Graphics and Interactive Techniques*, SIGGRAPH '99, pages 317–324. ACM Press/Addison-Wesley Publishing Co., 1999.

[8] Manfredo P. Do Carmo. *Differential Geometry of Curves and Surfaces*. Prentice-Hall, 1976.

[9] Tevian Dray. The hodge dual operator. Department of Mathematics, Oregon State University, 1999.

[10] Dominic G.B. Edelen. *Applied Exterior Calculus*. John Wiley & Sons, 1985.

[11] Douglas R. Farenick and Barbara A.F. Pidkowich. The spectral theorem in quaternions. *Linear Algebra and its Applications*, 371(0):75 – 102, 2003.

[12] Fernando de Goes, Pooran Memari, Patrick Mullen, and Mathieu Desbrun. Weighted Triangulations for Geometry Processing. *ACM Trans. Graph.*, 33(3):28:1–28:13, 2014.

[13] George Kamberov, Peter Norman, Franz Pedit, and Ulrich Pinkall. *Quaternions, Spinors and Surfaces*. American Mathematical Society, 2002.

[14] George Kamberov, Franz Pedit, and Ulrich Pinkall. Bonnet pairs and isothermic surfaces. *Duke Math. J.*, 92(3):637–644, 1998.

[15] Wolfgang Kühnel. *Differential Geometry*. American Mathematical Society, 2. edition, 2005.

[16] Yaron Lipman, Daniel Cohen-Or, Ran Gal, and David Levin. Volume and Shape Preservation via Moving Frame Manipulation. *ACM Trans. Graph.*, 26(1), 2007.

[17] Facundo Mémoli. Gromov–Wasserstein Distances and the Metric Approach to Object Matching. *Foundations of Computational Mathematics*, 11(4):417–487, 2011.

[18] Maks Ovsjanikov, Mirela Ben-Chen, Justin Solomon, Adrian Butscher, and Leonidas Guibas. Functional Maps: A Flexible Representation of Maps Between Shapes. *ACM Trans. Graph.*, 31(4):30:1–30:11, 2012.

[19] Maks Ovsjanikov, Jian Sun, and Leonidas Guibas. Global Intrinsic Symmetries of Shapes. In *Proceedings of the Symposium on Geometry Processing*, SGP '08, pages 1341–1348, 2008.

[20] Ulrich Pinkall and Konrad Polthier. Computing Discrete Minimal Surfaces and Their Conjugates. *Experimental Mathematics*, 2(1):15–36, 1993.

[21] Emanuele Rodolà, Andrea Torsello, Tatsuya Harada, Yasuo Kuniyoshi, and Daniel Cremers. Elastic Net Constraints for Shape Matching. In *Computer Vision (ICCV), 2013 IEEE International Conference on*, pages 1169–1176, 2013.

[22] Steven Rosenberg. *The Laplacian on a Riemannian Manifold*. Cambridge University Press, 1997.

[23] Raif M. Rustamov. Laplace-Beltrami Eigenfunctions for Deformation Invariant Shape Representation. In *Proceedings of the Fifth Eurographics Symposium on Geometry Processing*, SGP '07, pages 225–233, 2007.

[24] Jian Sun, Maks Ovsjanikov, and Leonidas Guibas. A Concise and Provably Informative Multi-Scale Signature Based on Heat Diffusion. *Computer Graphics Forum*, 28(5):1467–8659, 2009.

[25] Viswanath. Normal operators on quaternionic Hilbert spaces. *Trans. Amer. Math. Soc.*, 162:337–350, 1971.

[26] Max Wardetzky. Convergence of the Cotangent Formula: An Overview. In *Discrete Differential Geometry*, volume 38 of *Oberwolfach Seminars*, pages 275–286. Birkhäuser Basel, 2008.

[27] Max Wardetzky, Saurabh Mathur, Felix Kälberer, and Eitan Grinspun. Discrete Laplace Operators: No Free Lunch. In *Proceedings of the Fifth Eurographics Symposium on Geometry Processing*, SGP '07, pages 33–37, 2007.

[28] Wei Zeng, Ren Guo, Feng Luo, and Xianfeng Gu. Discrete Heat Kernel Determines Discrete Riemannian Metric. *Graphical Models*, 74(4):121–129, 2012.